

AD_____

Award Number: DAMD17-01-1-0410

TITLE: Molecular Characteristics of Multicorn, a New Large
Proteolytic Assembly and Potential Anti-Cancer Drug
Target, in Human Breast Cancer Cells

PRINCIPAL INVESTIGATOR: Maria E. Gaczynska, Ph.D.

CONTRACTING ORGANIZATION: The University of Texas Health Sciences
Center at San Antonio
San Antonio, TX 78229-3900

REPORT DATE: May 2005

TYPE OF REPORT: Final

20060215 144

PREPARED FOR: U.S. Army Medical Research and Materiel Command
Fort Detrick, Maryland 21702-5012

DISTRIBUTION STATEMENT: Approved for Public Release;
Distribution Unlimited

The views, opinions and/or findings contained in this report are
those of the author(s) and should not be construed as an official
Department of the Army position, policy or decision unless so
designated by other documentation.

REPORT DOCUMENTATION PAGE

Form Approved
OMB No. 074-0188

Public reporting burden for this collection of information is estimated to average 1 hour per response, including the time for reviewing instructions, searching existing data sources, gathering and maintaining the data needed, and completing and reviewing this collection of information. Send comments regarding this burden estimate or any other aspect of this collection of information, including suggestions for reducing this burden to Washington Headquarters Services, Directorate for Information Operations and Reports, 1215 Jefferson Davis Highway, Suite 1204, Arlington, VA 22202-4302, and to the Office of Management and Budget, Paperwork Reduction Project (0704-0188), Washington, DC 20503

1. AGENCY USE ONLY <i>(Leave blank)</i>			2. REPORT DATE May 2005	3. REPORT TYPE AND DATES COVERED Final (1 May 2001 - 30 Apr 2005)
4. TITLE AND SUBTITLE Molecular Characteristics of Multicorn, a New Large Proteolytic Assembly and Potential Anti-Cancer Drug Target, in Human Breast Cancer Cells			5. FUNDING NUMBERS DAMD17-01-1-0410	
6. AUTHOR(S) Maria E. Gaczynska, Ph.D.				
7. PERFORMING ORGANIZATION NAME(S) AND ADDRESS(ES) The University of Texas Health Sciences Center at San Antonio San Antonio, TX 78229-3900 <i>E-Mail:</i> gaczynska@uthscsa.edu			8. PERFORMING ORGANIZATION REPORT NUMBER	
9. SPONSORING / MONITORING AGENCY NAME(S) AND ADDRESS(ES) U.S. Army Medical Research and Materiel Command Fort Detrick, Maryland 21702-5012			10. SPONSORING / MONITORING AGENCY REPORT NUMBER	
11. SUPPLEMENTARY NOTES				
12a. DISTRIBUTION / AVAILABILITY STATEMENT Approved for Public Release; Distribution Unlimited			12b. DISTRIBUTION CODE	
13. ABSTRACT (Maximum 200 Words) Proper regulation of cell division and cell differentiation are the major factors preventing the neoplastic growth. Proteolysis is one of the widely accepted controlling mechanisms of these processes. The proteasome is the best known executor of controlled proteolysis in human cells. We discovered and biochemically characterized the multicorn, a giant proteolytic complex distinct from the proteasome. We found the multicorn to be identical with tripeptidyl peptidase II (TPP II), a ubiquitous eukaryotic protease of obscure functions. We found cell cycle-dependent differences in modifications and subcellular localization of TPP II in human breast cancer MCF-7 cells, as compared with non-cancerous MCF-10A cells. The total activity of TPP II seems to be several-fold lower in cancerous cells than in control cells. These intriguing observations suggest a likely involvement of TPP II in cell cycle progression, a novel notion about the protease. Most importantly, we observed that cancerous cells are much more vulnerable than control cells to cell death induced by the combined treatment with low doses of inhibitors of the proteasome and TPP II. Our findings confirm that the TPP II, most likely together with the proteasome, can be a useful anti-cancer drug target and a marker of neoplastic transformation.				
14. SUBJECT TERMS No subject terms provided.			15. NUMBER OF PAGES 44	
			16. PRICE CODE	
17. SECURITY CLASSIFICATION OF REPORT Unclassified	18. SECURITY CLASSIFICATION OF THIS PAGE Unclassified	19. SECURITY CLASSIFICATION OF ABSTRACT Unclassified	20. LIMITATION OF ABSTRACT Unlimited	

Table of Contents

Cover.....	1
SF 298.....	2
Table of Contents.....	3
Introduction.....	4
Body.....	5
Key Research Accomplishments.....	12
Reportable Outcomes.....	12
Conclusions.....	14
References.....	14
Appendices.....	17

INTRODUCTION

Proper regulation of cell division and cell differentiation are the major factors preventing the neoplastic growth. Proteolysis performed by the ubiquitin-proteasome pathway is one of the widely accepted controlling mechanisms of these processes. The proteasome is the major protease of the pathway and inhibition of its actions leads to apoptosis. One of specific inhibitors of the proteasome, bortezomib, is already approved to treat multiple myeloma and is under extensive clinical trials against other cancers, including breast cancer (Adams, 2002; Rajkumar et al., 2005). We have discovered that a giant proteolytic complex distinct from the proteasome is involved in partial overcoming the physiological effects of proteasome inhibitors (Glass et al., 1998). In subsequent studies we isolated and characterized an enzyme of nearly identical features from fission yeast and we named it multicore (Osmulski and Gaczynska, 1998). We found that the enzyme takes part in the cell cycle regulation (Osmulski and Gaczynska, 1998). The potential role in cell division combined with the proteasome-helping functions rendered the protease in human cells an attractive subject of studies as the potential anti-cancer drug target. As the biochemical and cell biology studies on the fission yeast and human protease advanced, the sequencing of the enzyme's subunit did not bring clear results and the multicore gene remained elusive. In the meantime, a homooligomeric tripeptidyl peptidase II (TPP II; EC 3.4.14.10) was postulated to take part in the previously reported overcoming the physiological effects of proteasome inhibitors (Geier et al., 1999; Princiotta et al., 2001). The research on TPP II took a separate route from our studies on the multicore, with a focus on processing of antigenic peptides (Reits et al., 2004; Seifert et al., 2003). Limited biochemical studies on TPP II took parallel routes to our studies on human multicore without clear indication if the enzymes are actually the same (Tomkinson, 2000). Finally, our recent preliminary data have shown that one of the variants of multicore-like protease subunit is identical with the TPP II subunit. Confirmation for other variants of the subunit is in progress. Identification of the multicore protease as TPP II adds an important body of biochemical and functional research to the knowledge about TPP II and places the enzyme as the second most prominent player in the controlled proteolysis after the proteasome. One of the most important data we obtained show that cancerous cells are much more vulnerable than the control cells to cell death induced by the synergistic action of the inhibitors of the TPP II and proteasome activities (described in submitted for publication manuscript, attached as Appendix 1). We found significant differences in the activity, amount, oligomerization status, posttranslational modifications and subcellular localization of TPP II in human breast cancer MCF-7 cells, as compared to noncancerous MCF-10A cells (described below and in a manuscript attached as Appendix 2). Notably, we found the total activity of the TPP II to be several-fold lower in cancerous cells than in control cells, and this result was confirmed with several methods, both *in vitro* and in living cells. With the help of a unique fluorogenic model substrate especially synthesized in our laboratory for studies in living cells, we observed that the proteolytically active TPP II congregates in the nuclear envelope on the onset of mitosis in noncancerous cells. In the carcinoma cells, however, the nuclear envelope localization was not limited to the onset of mitosis and was already prominent in G2 phase (Appendix 2). Our findings confirm that the TPP II, most likely together with the proteasome, can be a useful anti-cancer drug target and a marker of neoplastic transformation.

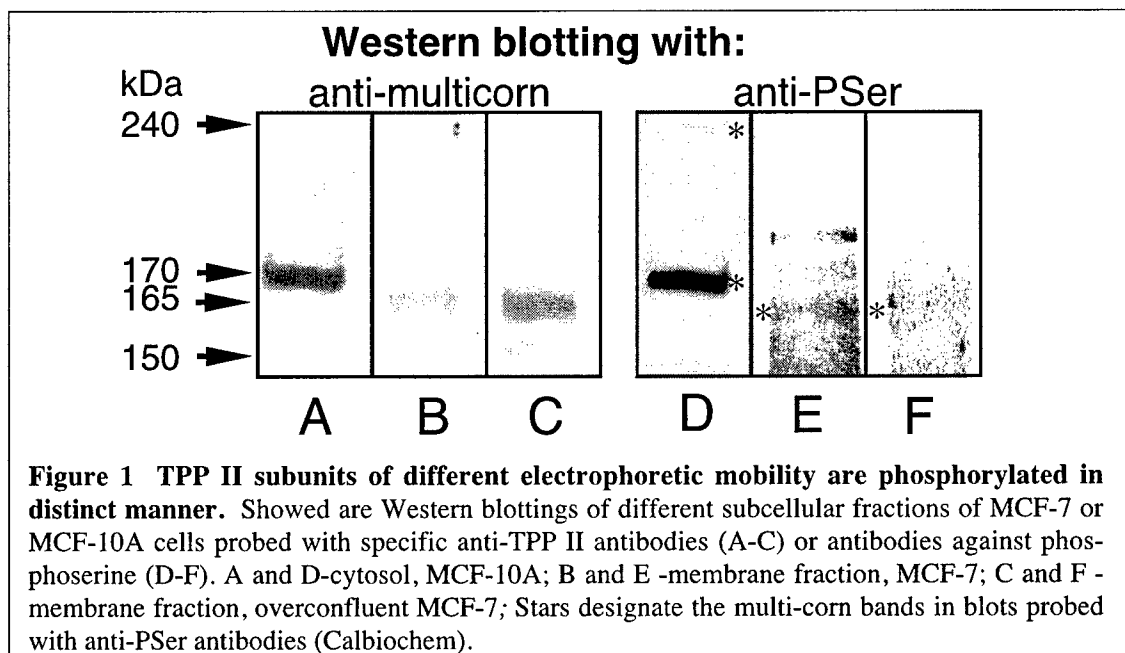
BODY

The research accomplishments associated with the objectives and tasks outlined in the approved Statement of Work are as follows:

Objective 1. Cloning and expressing the gene of human multicorn monomer.

Task 1: months 1 - 12; molecular basis of different physical and chemical properties of the two multicorn subunits will be studied using a combination of peptide mapping, sequencing and mass spectroscopy.

The task has been completed. We established that phosphorylation constitutes molecular basis of differences between several variants of the subunits (Figure 1). The 150 kDa subunit can be phosphorylated on several distinct serine residues to render polypeptides of electrophoretic mobilities of 165 kDa, 170 kDa and 240 kDa. We suspect that the 150 kDa protein is a phosphorylated (or, less likely, modified in some other way) version of the 138 kDa TPP II protein, but this modification was not recognized by the anti-phosphopeptide antibodies used. Further mass spectroscopy studies will likely answer the question. The reason why phosphorylation of TPP II have not been reported before may be related to high activity of dephosphorylating enzymes in crude cellular lysate. In our preparations, we routinely either added inhibitors of phosphatases (see also Appendix 2) or carried out the purification as quickly as possible and with the sample on ice all the time. We observed that when this regime was not followed, the 150 kDa subunit remained the major or the only protein in pure TPP II preparation, most likely due to a rapid dephosphorylation.



Task 2: months 1 - 6; cloning the gene, or genes, encoding the human multicorn monomers using HeLa cDNA library and PCR technology. It will be determined if the two types of subunits are encoded by the same gene.

The task has been abandoned. Instead, we determined that the 170 kDa protein has sequences identical with the tripeptidyl peptidase II (TPP II) subunit (see below). Therefore, we assume that the human multicorn and TPP II are, in fact, the same enzyme. The gene of human TPP II has been cloned before, rendering this task obsolete (Tomkinson and Jonsson, 1991). Interestingly, the TPP II or its close homologs have been found not only in vertebrates, but also in insects, plants and fission yeast (Tomkinson and Jonsson, 1991).

Identification of TPPII as the high molecular weight peptidase hydrolyzing AAF-MCA substrate using mass spectroscopy. Cytosolic multicorn was purified from MCF7 cells as described before using a combination of ultracentrifugation, anion exchange, and gel filtration chromatography. Fractions containing multicorn were pooled and concentrated on a membrane centrifugal concentrator. Subsequently, the sample was fractionated with 6% SDS PAGE. After Coomassie staining the 150kDa band containing the dominating subunit of multicorn was cut out from the gel, destained and processed for proteolytic digest and mass spectroscopy analysis. A standard procedure of Rosenfeld (1992) and Hellman (1995) was used to obtain peptides suitable for analysis with MALDI-TOF. In short, the excised piece of gel was destained and dehydrated. Next, the sample was reduced with 10mM DDT and alkylated with 55mM IAA, washed, and transferred to trypsin solution (10 μ g/mL, Promega). The sample was digested at 37°C for 16hrs. Resulting peptides were extracted and desalted using C18 ZipTips (Millipore). Finally, the sample was mixed with a matrix and analyzed with MALDI-TOF Voyager (ABI) in a range of masses 500 to 5,000Da. For the database match search, we considered the following protein modifications: peptide N-terminal glutamine to pyroglutamic transformation, oxidation of methionine, acetylation of protein N-terminus, and phosphorylation of serine, threonine and tyrosine residues. The obtained so far spectra allowed us to identify the 150kDa band as representing protein similar or identical with human tripeptidyl peptidase II (TPPII) with a sequence of 1249 amino acids, accession number CAH72179, GI:55661755, derived from the embl accession AL158063.12. The sequence of this peptidase and matching peptides from the MALDI-TOF analysis is shown below:

1	11	21	31	41	51	61	71
MATAATEEPP	PFHGLLPKKE	TGAASFLCRY	PEYDGRGVLI	AVLDTGVDPG	APGMQVTTDG	KPKIVDIDI	TGSGDVNTAT
81	91	101	111	121	131	141	151
EVEPKDCEV	GLSGRVLKIP	ASWTNPSSKY	HIGIKNGYDF	YPKALKERIQ	KERKEKIKWDP	VHRVALAEAC	RKQEEFDVAN
161	171	181	191	201	211	221	231
NGSSANKLH	KEELQSQVEL	LNSFEKKYSD	PGPVYDCLW	HDGEVWRACI	DSNEUDGLSK	STVLRNYKREA	QEYGSFGTAE
241	251	261	271	281	291	301	311
MLNYSVNIYD	DGNLLSIVTS	GGAHGTHVAS	IAAGHFFPEP	ERNGVAPGAQ	IILSIKIGDTR	LSTWETGTGL	IRAMIEVINH
321	331	341	351	361	371	381	391
KCDLVNYSYG	EATHWPNSGR	ICEVINEAVW	KHNIIYVSSA	GNNGPCLSTY	GCPGGTSSV	IGVGAYVSPD	MMVAEYSLRE
401	411	421	431	441	451	461	471
KLPANQYNTS	SRGSPADGAL	GVSISAPGGA	IASVPNWTLR	GTQLMNGTSM	SSPNACGGIA	LILSGKLANN	IDYTVHSVRA
481	491	501	511	521	531	541	551
ALENTAVKAD	NIEVFAQQHGK	IIOQVOKAYDY	LWQNTSFANK	LGFTVTVGNR	RGIYLRDPVQ	VAAPSHHGCG	IEFVPPENTE
561	571	581	591	601	611	621	631
NSEKISLQLH	LALTNSSSWV	QCPSHLELMN	QCRHINIRVD	PRGLREGLHY	TEVCGYDIAS	PNAGPLFRVP	ITAVIAAKVN
641	651	661	671	681	691	701	711
ESSHYDLAFT	DVHFPGQIR	RHFIEVPEGV	TWAEVTCSC	SSEVSARFVL	HAVQLVQRA	YRSHEFYKFC	SLPERGTILTE
721	731	741	751	761	771	781	791
APFVLGGKAI	EFCIARWWAS	LSDVNIDYTT	SFHGIVCTAP	QLNIHASEGI	NRFDVQSSLK	YEDLAPCITL	KNWVQTLRPV
801	811	821	831	841	851	861	871
SAKTKPLGSR	DVLPNRRQLY	EMVLTYNFHQ	PRSGEVTIPSC	PLLCELVYES	EFDSDOLIIF	DQNRKRQMGSG	DAYPHQYSLK
881	891	901	911	921	931	941	951
LIKGDYTIKL	QIRHEQISDL	ERLKDLPPFIV	SHRLSNTLSL	DIHENHSFAL	LGKKKSSNL	LPPKYNQPPF	VTSLPPDDKIP

961	971	981	991	1001	1011	1021	1031
KGAGPGCYLA	GSITLSKTEL	GGKAKDVIPIH	YELIPPEFTK	RNGGRDKEKD	SEKEKDKEE	FTEARDLKI	QWMYTKLDSSD
1041	1051	1061	1071	1081	1091	1101	1111
LYNELKETYP	NYLPLYVARL	HOLDAEKERG	YELIPPEFTK	YANVSHIDDT	ALAWYIANKT	DPRPDAATIK	NDMDKQKSTL
1121	1131	1141	1151	1161	1171	1181	1191
UDALCRKGCA	LADHLLHTQA	QDGAISTDAE	GKEEEGESPL	DSLAEITFWET	TKWTDILFDNK	VIITPAYHAL	VNNRIGKGKIK
1201	1211	1221	1231	1241			
PATEKILVERDEKE							
TKENWKNCIO							
LMKLLGWTHC							
ASPTENWLPI							
MYPDPDYCVF							

The current coverage of the sequence is about 10% and is mostly clustered at the C-terminal portion of the protein. Since no other digest times were attempted, nor other modifications considered, there is a possibility that such an uneven coverage may result from not complete digest of relatively large protein and/or its additional modification of unknown type interfering with efficient trypsin digestion. Interestingly, we were able to identify two pairs of peptides with possible sites of phosphorylation modification:

- 1) 1181-1197 (2 or no phosphorylation)
- 2) 1198-1212 (1 or 2 phosphorylation sites).

Additionally, a peptide 1070-1099 was identified as bearing oxidized methionine residue. We plan to analyze in a similar way other bands identified previously with the specific antibodies as representing multicorn. We will also attempt to remove phosphate groups from the all of the modified residues using a phosphatase of a broad specificity to simplify sequence analysis and test our current hypothesis of highly complex posttranslational modifications of TPPII.

Task 3: months 6 - 18; expressing the gene(s) in *Schizosaccharomyces pombe* or mammalian expression system. The goal of this task is to obtain active recombinant TPP II molecules characterized by controlled content of the specific monomers.

The task was abandoned in the light of finding that the human multicorn and TPP II are the same enzyme, as outlined above. The last-minute timing of identification of the multicorn protease as TPP II prevented from asking for permission to modify the SOW. A more extensive biochemical characterization of the TPP II was carried out instead the two above tasks (see below).

Objective 2. Studying the mechanism controlling the multicorn activity through its oligomerization and phosphorylation.

Task 1: months 6 - 24; The multicorn complexes of different supramolecular organization and posttranslational modifications will be separated and purified. The qualitative and quantitative parameters of proteolysis catalyzed by these distinct complexes will be determined using selected protein substrates and model fluorogenic peptide substrates.

The task has been completed. We found that the large form of the TPP II (about 4,000 kDa) is built mostly from the 170 kDa and small amounts of the 165 kDa and 240 kDa phosphorylated forms of the 150 kDa TPP II subunit. We found that the small form of the TPP II (900 kDa) is assembled mostly from the phosphorylated 240 kDa and non-phosphorylated 150 kDa polypeptides, and trace amounts of the phosphorylated 170 kDa

protein. We identified the 170 kDa form as the one responsible for the proteolytic activity. We carried out further biochemical characterization of purified human TPP II.

We purified the two oligomeric forms by a set of differential centrifugations combined with gel filtration and anion exchange chromatography (Gaczynska et al., 1993; Glas et al, 1998). Specifically, we enriched the cytosolic fractions of the cells with the large protein assemblies using 5 – hour ultracentrifugation at 100,000xg (at 4°C). The resulting high molecular weight protein pellet was resolubilized and subjected to gel filtration chromatography on a Superose 6 column (Pharmacia), especially designed for the separation of the large biomacromolecules with high resolution (Osmulski and Gaczynska, 1998). Activity of the protease was detected in profiles by incubation with fluorogenic model peptide substrate AlaAlaPhe-7-amino-4-methylcoumarine (AAF-MCA). The applied procedure produced fractions containing about 80% pure large form (eluted at 6.5 – 7.5 ml), and fractions containing about 20% of the small form (eluted at 9.5 – 11 ml, *Figure 2*). Further purification of TPP II was carried out by anion exchange chromatography on the HQ/M column (Applied Biosystems). Identity of the isolated oligomeric forms was confirmed on Western blots probed with the specific polyclonal antibodies (*Figure 3*). Electrophoretically pure oligomers of TPP II were obtained as a result.

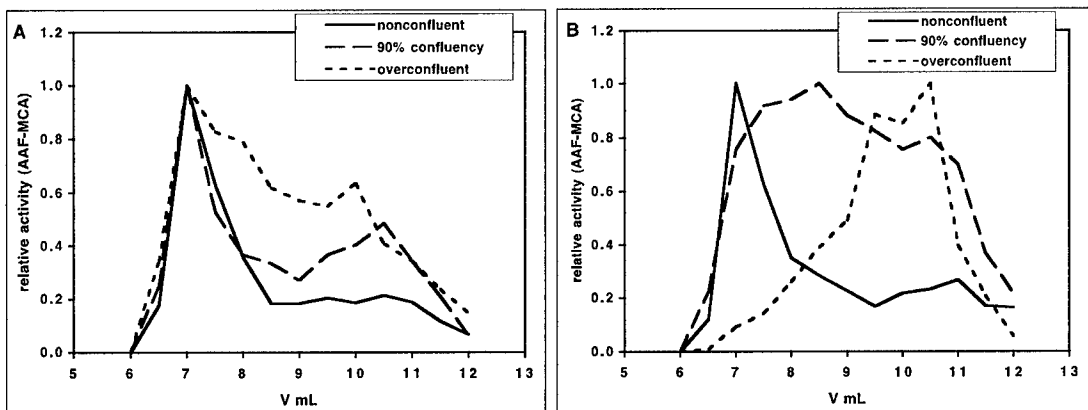


Figure 2. Gel filtration profiles of peptidase activity measured with AAF-MCA in 5hr pellet fractions of (A) MCF-7 and (B) MCF-10A. The cells were harvested as non-confluent, subconfluent (90%) or overconfluent. The activity profiles show presence of two major forms of the multicore: the large form is eluted at 6.5-7.5 mL and small form at 9.5-11 mL. The increase of cell culture density shifted the equilibrium between forms from the dominance of the large form to the dominance of the small form in MCF-10A cell. MCF-7 cells show a very limited shift under similar conditions. The activities are standarized for each profile against the highest value of activity in the profile.

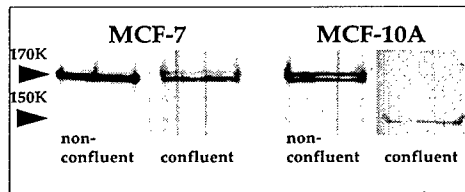


Figure 3. The large form of TPP II from MCF-7 human breast cancer cells is composed mostly from the 170 kDa subunit in both confluent (G_0) and non-confluent cells. The large form from non-cancerous MCF-10A cells is composed mostly from

170 kDa subunit or 150 kDa subunit, depending on confluence. Silver stained SDS-PAGE (8% acrylamide) gel with partially purified (95%) large forms of TPP II is shown. Total activity of the protease was the lowest in confluent (G_0) MCF-10A cells, and the highest in non-confluent MCF-7 cells. Just to the opposite, specific activity was the highest in confluent MCF-10A cells.

The large forms of TPP II isolated from the two cell lines differed about two - fold in their content of the 170 kDa phosphorylated subunit (Figure 4). We suspect that the 170 kDa subunit is responsible for most of the activity detected with the model peptide substrate, AAF-MCA. Still, the two - fold difference in the protein content could hardly account for the six - fold difference in the TPP II activity. There are several probable explanations for this finding. It is possible that the 170 kDa subunit plays slightly different roles in the large forms resulting in their distinct specific activities. The large forms, although eluted at the same volume, are likely organized differently in the two cell lines. The reason for the detection of very little of the TPP II activity in the MCF-7 cells may lay in its lower stability. Obviously, some other factors, perhaps the content of other, differently phosphorylated subunits, may also modulate the specific activity of the large form. The presence of several oligomeric forms of TPP II has been reported before, however the small form was not characterized in detail in other studies (Tomkinson, 2000).

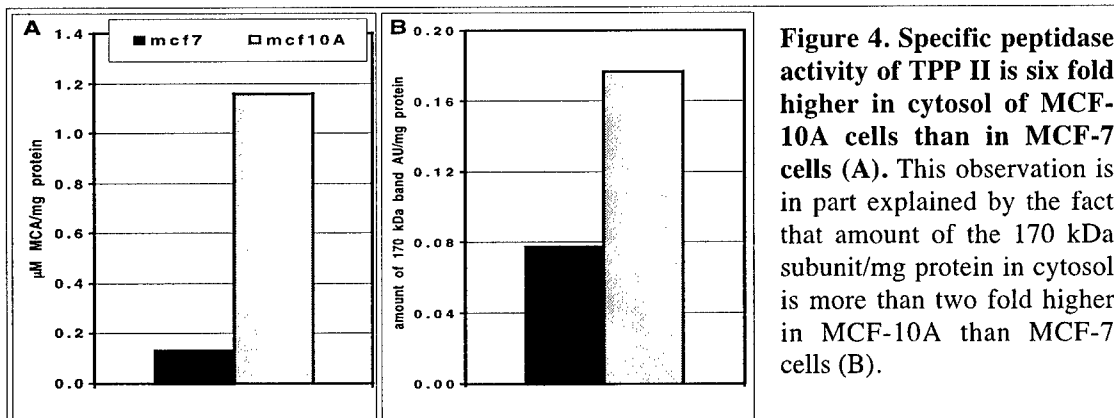


Figure 4. Specific peptidase activity of TPP II is six fold higher in cytosol of MCF-10A cells than in MCF-7 cells (A). This observation is in part explained by the fact that amount of the 170 kDa subunit/mg protein in cytosol is more than two fold higher in MCF-10A than MCF-7 cells (B).

Additionally, we determined proteolytic capabilities of both forms purified from the cytosol of MCF-7 cells. In addition to the commonly used AAF-MCA substrate, both forms degraded AFK-MCA (AlaPheLys-methylcoumarin) and GPL- β NA (GlyProLeu- β -naphthylamide) fluorogenic substrates. The results confirmed the broad tripeptidyl specificity of the protease and showed that even peptides containing proline can be cleaved off by TPP II, the latter peptides considered before not to be good substrates (Tomkinson and Lindas, 2005). We also tested if both forms of TPP II possess an endopeptidase activity, as postulated by (Geier et al., 1999). We incubated purified large and small forms of TPP II with previously reduced lysozyme or lactalbumin (Osmulski and Gaczynska, 1998), at 37°C for 3 or 9 hours. After incubation the samples were run on 15% SDS-PAGE, stained with Coomassie Blue and analyzed for the presence of products of degradation. Alternatively, the samples were run on reverse-phase HPLC column, as described in (Osmulski and Gaczynska, 1998). Both methods revealed that the large form is capable to degrade lysozyme and lactalbumin, whereas the products of degradation were not detectable for the small form of TPP II.

Objective 3. Molecular characterization of the multicorn at different stages of the cell cycle.

Task 1: months 12 - 18; we will perform flow cytometric analysis of nonsynchronous MCF-7 and MCF-10A cells stained with anti-multicorn antibodies and with propidium iodide (DNA).

The task has been completed, with a modification that brought substantially more data than originally planned, as described below and in Appendices 1 and 2.

We decided to study level and localization of TPP II in the cells by tracing hydrolysis of its model fluorogenic peptide substrate AAF-CMAC (AlaAlaPhe-7-amino-4-chloromethylcoumarin) using fluorescence microscopy instead of previously planned flow cytometry. The results of our studies, complete with a model of dynamic subcellular localization of TPP II, are described in Appendix 2 (submitted for publication). We are confident that analysis of the actual activity of the protease inside living cells is more informative than the originally planned analysis of the expression level of the TPP II subunit. In short, AlaAlaPhe-7-amino-4-chloromethylcoumarin (AAF-CMAC) and succinylLeuLeuValTyr-chloromethylcoumarin (SucLLVY-CMAC) were used to monitor in living cultured cells the activity of the TPP II and the proteasome, respectively. Both substrates were synthesized in our laboratory, as described in Appendix 2. The CMAC (chloromethylcoumarin) label is characterized by a substantially better retention in living cells and much lower diffusion rate than the commonly used MCA (methylcoumarin) label, without sacrificing a yield of fluorescence and solubility in water-based solvents. CMAC labeled substrates are practically not available commercially. We established a reliable quantification method of the TPP II and proteasome activities on the basis of images collected with fluorescence microscopy. Using free CMAC solution of a known concentration (5 - 10 nM) as a standard, we quantified the mean pixel intensities for images integrated at different times. For example, the integration time *versus* intensity plots for 5 nM standard displayed two regions of linearity, for integration times from 1 to about 250 ms and then from 300 ms to 1 s. Based on these standard plots, we determined that nuclei of nonsynchronous MCF-10A cells display on average 6-fold higher activity of the TPP II than nuclei of MCF-7 cells. In contrast, peptidase activity in the corresponding cytosols differed only up to 3-fold.

Moreover, we decided to supplement the characterization of the role of TPP II by studies of cells treated by the inhibitor of the TPP II, by the inhibitor of the proteasome, and by a combination of both inhibitors. The rationale supporting these experiments was a long suspected functional coupling of the TPP II and the proteasome, which is an acknowledged anticancer drug target and a major intracellular protease (Glas et al., 1998). The results of these very successful experiments are described in Appendix 1 (submitted for publication). In short, we compared effects of treatment of the control and cancerous cell lines with MG262 or AAF-CMK (AlaAlaPhe-chloromethylketone) alone or in mixtures at different concentrations. MG262 is a high-affinity, specific inhibitor of the proteasome, and a close homologue of the approved anti-cancer drug bortezomib (Adams, J., 2002;.Gaczynska and Osmulski, 2005). AAF-CMK, on the other hand, is the

specific inhibitor of TPP II. As expected, treatment with MG262 was more toxic for the cancerous than the noncancerous breast cells. Treatment with AAF-CMK, on the other hand, was toxic for both cell lines with a preference for the noncancerous cells. The two compounds used together acted synergistically to promote apoptosis in both MCF-7 and MCF-10A cells. However, we found combination of doses of both drugs which preferentially kill cancerous cells, leaving substantial fraction of the noncancerous cells viable. The combination was more efficient in differentiating between cancerous and noncancerous cells than the proteasomal inhibitor alone (Appendix 1). This result indicates that simultaneous targeting the proteasome and TPP II may be a viable strategy to specifically cause apoptosis in cancerous cells, especially cells which are relatively less sensitive to inhibition of the proteasome, like MCF-7 cells (An et al., 2000; Teicher et al., 1999); Appendix 1.

Task 2: months 18 - 36; we will analyze the expression and biochemical properties of the TPP II in synchronized MCF-7 and MCF-10A cells.

The task has been completed and the results are described in Appendix 2. We found that the proteolytically active, phosphorylated large form of the TPP II localized mostly in the cytosol, and also in the nuclear envelope. To the contrary, cells in G₀ exhibited only a weak cytosolic activity of the protease. The cancerous MCF-7 cells exhibited several-fold lower TPP II activity than the control noncancerous MCF-10A cells. During mitosis the TPP II activity apparently colocalized with the emerging chromosomes. Interestingly, the dramatic shift of major localization of the TPP II activity from cytosolic to nuclear envelope was a feature of the control cells and not the cancerous cells. In the latter the TPP II activity was detectable both in the cytosol and around nucleus already in G2 phase (Appendix 2).

KEY RESEARCH ACCOMPLISHMENTS

The major accomplishments of this study:

- **identification of the human multicorn protease as tripeptidyl peptidase II by mass spectroscopy;**
- **biochemical characterization of the TPP II in human breast cells, including discovery of a multiple phosphorylation of TPP II subunit; the phosphorylation regulates activity and oligomerization and potentially also subcellular localization of TPP II (a manuscript pending completion of identification of phosphorylation sites);**
- **synthesizing a specific model substrate and establishing conditions for observation of the TPP II activity in living cells (Appendix 2);**
- **discovering cell cycle-related differences in structure, function and subcellular localization of the protease, strongly suggesting its involvement in cell cycle progression (Appendix 2);**
- **discovering significant differences between activity and subcellular localization of the TPP II in cancerous and noncancerous human breast cells, suggesting a potential use of the protease as marker of neoplastic transformation (Appendix 2);**
- **discovering synergistic pro-apoptotic effects of combined inhibitors of the proteasome and TPP II on human breast cancer cells; the combination of drugs acts better than a proteasome inhibitor alone to preferentially kill cancerous cells and leave noncancerous cells viable (Appendix 1).**

REPORTABLE OUTCOME

1. The research conducted on the project was a topic of the following posters/plenary talks (abstracts, when available, are attached in APPENDICES):

- **“Cancer, proteases and proteolytic instability.”** poster by Pawel A. Osmulski, Xianzhi Jang, Bingnan Gu and Maria E Gaczynska, presented on 12th Annual Symposium on Cancer Research in San Antonio (July 12th, 2002);
- **“Proteolytic instability in breast cancer cells”** poster (by Maria E Gaczynska, Xianzhi Jang, Bingnan Gu, Pawel A. Osmulski), and a plenary talk (Gaczynska) presented on the Era of Hope DOD Breast Cancer Research Program Meeting (Orlando, September 25-28, 2002);

- “**Proteolytic instability in breast cancer cells.**” poster by Pawel A. Osmulski, Xianzhi Jang, Bingnan Gu and Maria E. Gaczynska, presented on 2nd International Symposium on Cancer Research “Frontiers in Cancer Research: a Molecular Perspective” (San Antonio, October 12-14, 2002);
- “**Synergistic action of inhibitors of large cytosolic proteases on breast cancer cells.**” poster by Gaczynska M., Jankowska E., Osmulski P.A., presented on 13th Annual Symposium on Cancer Research in San Antonio and South Texas (November 11th, 2004);
- “**Proteasome-related molecular signature of breast cancer**” poster by Brett Mueller, Pawel A. Osmulski and Maria Gaczynska, presented on Annual Retreat of San Antonio Cancer Institute/Genomic Integrity and Carcinogenesis Program (May 25, 2005). Presenter Brett Mueller was awarded a 2nd price in the technician category during a poster competition.
- “**A high-throughput-agarose gel electrophoresis based method for comparing proteasomes in normal and cancerous cells.**” poster by Xiaolin Tan, Maria Gaczynska and Pawel A. Osmulski, presented on Annual Retreat of San Antonio Cancer Institute/Genomic Integrity and Carcinogenesis Program (May 25, 2005). Presenter Xiaolin Tan was awarded a 2nd price in the graduate student category during a poster competition.
- “**Inhibitors of large cytosolic proteases act synergistically to kill breast cancer cells.**” poster by Maria Gaczynska and Pawel A. Osmulski, will be presented on the Era of Hope DOD Breast Cancer Research Program Meeting (Philadelphia, June 8-11, 2005).

2. The research conducted on the project was presented during the following invited lectures:

- “**The target and the bullets: aiming at the proteasome in cancer therapies.**” (M. Gaczynska), 13th Annual Symposium on Cancer Research in San Antonio (July 12th, 2002).
- “**Carpet bombing or sniper fire: the two approaches in proteasome-targeting drug development.**” (M. Gaczynska), Institute of Drug Development (San Antonio, January 22, 2003).
- “**Caretaker or Undertaker: The Role of The Proteasome/Ubiquitin System in Aging**” (M. Gaczynska), The Spring 2004 Biology of Aging Seminar Series at The Barshop Center for Longevity and Aging Studies/The San Antonio Nathan Shock Aging Center.
- “**Regulation of the Proteasome**” (M. Gaczynska), Institute of Drug Development, San Antonio, May 11, 2005.

Two manuscripts submitted for publication (Molecular Cancer and Breast Cancer Research) are attached as Appendix 1 and Appendix 2. The third manuscript is pending and will be submitted as soon as the mass spectroscopy-based identification of phosphorylation sites will be completed. The now-ready data that will constitute the manuscript are included in this report.

CONCLUSIONS

We showed that breast cancer MCF-7 cells posses a distinct regulation of proteolysis executed by the TPP II when compared with non-cancerous MCF-10A cells. The apparent lower total activity of the TPP II in MCF-7 cells and only weak changes in subcellular localization may constitute an important link between the overall efficiency of cell division and nuclear and cytosolic proteolysis. Regulation of the assembly of the large and small forms of TPP II is accomplished through a complex phosphorylation pattern of their subunits. Moreover, it seems that the phosphorylation also controls subcellular localization of the TPP II and ultimately its fate. The cellular distribution of the TPP II, similarly to the best known large intracellular protease, the proteasome, is not limited to cytosol, however the most of the both proteases resides in this compartment. On the basis of our data we suspect that TPP II constitutes an important player in cellular protein turnover and in regulation of cell cycle. Its distinct properties in the control and cancerous cells strongly suggest that the TPP II may represent an attractive drug target and a marker of physiological state of the cells. Since it has been long suspected that both proteasome and the TPP II may share some of their functions, we tested the performance of cancerous and control cells treated with inhibitors of the proteasome, of the TPP II, and both the inhibitors combined. The results of these tests are very encouraging. High doses of TPP II and proteasome inhibitors are invariably toxic to the cells. However, we determined that a combination of low doses of both inhibitors effectively kills the cancerous cells allowing the noncancerous cells to recover. This result point at a potential practical use of mixed-inhibitor therapy and underlines the importance of comprehensive understanding of cellular controlled proteolysis.

REFERENCES

Adams, J. (2002). Development of the proteasome inhibitor PS-341, *Oncologist* 7, 9-16.

An, W. G., Hwang, S. G., Trepel, J. B., and Blagosklonny, M. V. (2000). Protease inhibitor-induced apoptosis: accumulation of wt p53, p21WAF1/CIP1, and induction of apoptosis are independent markers of proteasome inhibition, *Leukemia* 14, 1276-83.

Gaczynska, M., Osmulski, P.A (2005) "Small-molecule inhibitors of the proteasome activity." for the "Ubiquitin-Proteasome Protocols", Methods in Molecular Biology series, Patterson, C., Cyr, D.M., Editors, Humana Press, 3-22.

Geier, E., Pfeifer, G., Wilm, M., Lucchiari-Hartz, M., Baumeister, W., Eichmann, K., and Niedermann, G. (1999). A giant protease with potential to substitute for some functions of the proteasome, *Science* 283, 978-81.

Glas, R., Bogyo, M., McMaster, J. S., Gaczynska, M., and Ploegh, H. L. (1998). A proteolytic system that compensates for loss of proteasome function. *Nature* 392, 618-622.

Hellman U., Wernstedt C., Gómez J., and Heldin C. H. (1995) Improvement of an "In-Gel" Digestion Procedure for the Micropreparation of Internal Protein Fragments for Amino Acid Sequencing. *Anal. Biochem.*, 224, 451-455.

Osmulski, P. A., and Gaczynska, M. (1998). A new large proteolytic complex distinct from the proteasome is present in the cytosol of fission yeast, *Current Biology* 8, 1023-6.

Princiotta, M. F., Schubert, U., Chen, W. S., Bennink, J. R., Myung, J., Crews, C. M., and Yewdell, J. W. (2001). Cells adapted to the proteasome inhibitor 4-hydroxy5-iodo-3-nitrophenylacetyl-Leu-Leu-leucinal-vinyl sulfone require enzymatically active proteasomes for continued survival, *Proc Natl Acad Sci U S A* 98, 513-518.

Rajkumar, S. V., Richardson, P. G., Hidemitsu, T., and Anderson, K. C. (2005). Proteasome inhibition as a novel therapeutic target in human cancer, *Journal of Clinical Oncology* 23, 630-9.

Reits, E., Neijissen, J., Herberts, C., Benckhuijsen, W., Janssen, L., Drijfhout, J. W., and Neefjes, J. (2004). A major role for TPPII in trimming proteasomal degradation products for MHC class I antigen presentation., *Immunity* 20, 495-506.

Rosenfeld J., Capdevielle J., Guillemot J.C., and Ferrara P. (1992) In-gel digestion of proteins for internal sequence analysis after one- or two-dimensional gel electrophoresis. *Anal. Biochem.*, 203, 173-179.

Seifert, U., Maranon, C., Shmueli, A., Desoutter, J. F., Wesoloski, L., Janek, K., Henklein, P., Diescher, S., Andrieu, M., de la Salle, H., *et al.* (2003). An essential role for tripeptidyl peptidase in the generation of an MHC class I epitope., *Nature Immunology* 4, 375-9.

Teicher, B. A., Ara, G., Herbst, R., Palombella, V. J., and Adams, J. (1999). The proteasome inhibitor PS-341 in cancer therapy, *Clinical Cancer Research* 5, 2638-2645.

Tomkinson, B. (2000). Association and dissociation of the tripeptidyl-peptidase II complex as a way of regulating the enzyme activity, *Archives of Biochemistry & Biophysics* 376, 275-80.

Tomkinson, B., and Jonsson, A. K. (1991). Characterization of cDNA for human tripeptidyl peptidase II: the N-terminal part of the enzyme is similar to subtilisin, *Biochemistry* 30, 168-74.

Tomkinson, B., and Lindas, A. C. (2005). Tripeptidyl-peptidase II: A multi-purpose peptidase., *The International Journal of Biochemistry and Cell Biology* 37, 1933-1937.

APPENDIX 1

Breast cancer cells are specifically targeted by synergistic effects of proteasomal and TPP II inhibitors.

Pawel A. Osmulski and Maria Gaczynska

Contribution from:

Institute of Biotechnology, Department of Molecular Medicine, University of Texas Health Science Center at San Antonio
15355 Lambda Drive, San Antonio, TX 78245
contact:
e-mail: Gaczynska@uthscsa.edu, phones: office (210) 567-7262 laboratory (210) 567-7259,
(210) 567-7265, fax (210) 567-7269

Abstract

The ubiquitin-proteasome (UBP) pathway constitutes one of the key regulatory elements of the intracellular protein turnover. Inhibition of proteolysis performed by the proteasome, a central protease in the pathway, leads to a preferential apoptosis of cancerous cells. Although a detail mechanism of the distinct cellular response of cancerous cells has not been elucidated, a drug bortezomib utilizing this property is already used to treat multiple myeloma. In addition to the proteasome, there are several peptidases in the UBP pathway that participate in trimming or further degradation of the products released by the proteasomal activity. One of such peptidase which is currently gaining more scrutiny, is tripeptidyl peptidase II (TPPII). Here we show that inhibition of TPPII with AAF-CMK, its specific inhibitor, is toxic to both noncancerous MCF10A and cancerous MCF7 cells, therefore it is not pharmacologically relevant. However, the simultaneous treatment of the cells with AAF-CMK and MG262, a specific inhibitor of proteasome, leads to much more profound apoptosis of the MCF7 than MCF10A cells. Moreover, that effect is much stronger when compared to the result of the exposure of the cells to MG262 alone. Therefore, the synergistic action of the compounds is suspected, which influence the separate enzymes of the UBP pathway. It seems plausible to further investigate possible benefits arising from the apparent synergy between drugs interfering with the proteolytic activity of the UBP pathway.

Introduction

Controlled proteolysis performed by enzymes of the ubiquitin-proteasome (UBP) pathway is one of the major intracellular regulatory mechanisms (1). Therefore, it comes to no surprise that the controlled proteolysis is involved in such diverse processes as neoplastic transformation, tumor progression, drug resistance, or impaired immunosurveillance. The UBP regulates cell cycle progression, degrades oncogene and suppressor gene products, digests receptor proteins, and supplies antigenic peptides directly linked to cancer. The best-known cancer-related substrates of UBP, to name a few, are cyclins D and E, cyclin dependent kinase inhibitor p27, tumor suppressor proteins p53 and RB (retinoblastoma), and regulator of angiogenesis HIF-1 α (hypoxia-inducible factor 1 α) (2). In the notably case of I κ B α /NF κ B (nuclear factor kappa-B

and its inhibitor), the product of proteasomal cleavage is the actual active transcription factor, NF κ B (3). The best known proteasomal substrates involved specifically in breast cancer include an estrogen receptor, which is down regulated in breast cancer cells, and a breast cancer susceptibility gene product BRCA1, which itself is one of UBP enzymes (4, 5).

In short, the UBP consists of a cascade of enzymes recognizing unneeded or damaged proteins and marking them for degradation by attachment of multiple copies of a small protein ubiquitin. The proteasome, a multisubunit and multifunctional proteolytic enzyme, recognizes ubiquitinated proteins and cleaves them into peptides, recycling ubiquitin. The three pairs of active centers of the proteasome display chymotrypsin-like, trypsin-like and post-acidic endopeptidase activities to break peptide bonds after hydrophobic, basic and acidic amino acids, respectively. The products can be trimmed by downstream proteases and used as MHC (major histocompatibility complex) class I antigens or may be degraded to recyclable amino acids by aminopeptidases (6). One of well-documented proteases acting downstream of the proteasome is tripeptidyl peptidase II (TPP II), a giant homooligomeric cytosolic enzyme of broad specificity, processing products of the proteasomal degradation and delivering antigenic peptides or substrates for aminopeptidases (7, 8).

Inhibition of the proteasome activity inevitably leads to the cell death, therefore the UBP was not long ago considered an unlikely target for anti-cancer pharmacological intervention. The notion was invalidated with a discovery that cancer cells are generally more susceptible to apoptosis triggered by the proteasome inhibition than normal cells (9, 10). A small-molecule inhibitor of the leading chymotrypsin-like activity of the proteasome, a peptide boronic acid bortezomib (PS-341, VelcadeTM), was approved in a fast-tract process to treat multiple myeloma. Bortezomib is clinically tested for treatment of other cancers, including phase I and II trials for breast cancer (9, 10). The molecular basis of the crucial difference in susceptibility are not well understood. Differences in a general flux of substrates in normal cells versus rapidly proliferating cancerous cells and differences in the functioning of the UBP in both cases provide the most likely culprits. The bortezomib-induced apoptosis is believed to be mediated through inhibition of NF κ B (10).

The advantages of using proteasome inhibition in cancer therapy include relatively low toxicity and sensitization of transformed cells to other chemotherapeutic agents (10). Not all kinds of cancer cells, however, are equally sensitive to proteasome inhibitors. Very complex and not well understood inhibitor-induced cellular responses may be at least in part responsible for the observed differences. One of the responses is upregulation of yet other proteolytic enzyme, namely TPP II, observed in cells adapted to survive a prolonged treatment with proteasome inhibitors (11, 12). When the mouse EL-4 lymphoma cells were maintained in the presence of a toxic dose of a peptide vinyl sulfone (NLVS), an irreversible and competitive proteasome inhibitor, most of the cells died. However a small population outgrew and remained resistant to further treatment with the inhibitor (12). Another cell line, murine mastocytoma P815, was also amenable to the adaptation process as well, however with another proteasomal inhibitor, lactacystin, (11, 13). The adapted cells displayed residual activity of the proteasome, necessary for their ultimate survival (13). Interestingly, the activity of TPP II was several-fold upregulated in the adapted cells (11, 12). Moreover, overexpression of TPP II in EL-4 cells rendered them resistant to NLVS treatment without the prolonged adaptation process, leading to the notion that TPP II is able to substitute for some functions of the proteasome (14).

The suspected interplay between the proteasome and TPP II makes both proteases attractive targets for a joint treatment. If controlled proteolysis in cancer cells with proteasome

activity impaired by a drug rely at least in part on the TPP II actions, then simultaneous inhibition of both enzymes should deliver a deciding blow to the cells' physiology and initiate apoptosis. Combining chemotherapeutics to amplify the proapoptotic effects is a proven strategy in cancer treatment. For example, in preclinical and clinical studies of breast cancer bortezomib is tested together with taxanes or anthracyclines, which activate proapoptotic signaling through NF κ B and p44/42 MAPK pathways (9). However, the effects of a joint use of inhibitors for two distinct proteases from the UBP have not been compared so far in cancerous and noncancerous cells. The only experiments involving the proteasome and TPP II inhibitors involved adapted and non adapted cancer cells. In one study, a specific TPP II inhibitor, AAF-CMK (AlaAlaPhe-chloromethylketone), stopped growth of the adapted, but not control EL-4 cells (12). In another study, cytotoxic effects of this compound were similar for adapted and non adapted mouse lymphoma cells (13).

We decided to test the combined influence of a proteasomal inhibitor and inhibitor of the TPP II activity on the survival of cultured cells, apart from the phenomenon of adaptation. Instead, we compared the sensitivity of cancerous and noncancerous breast cells. The aim of this experiment was two-fold. Firstly, we wanted to test if mixtures of the inhibitors show synergistic cytotoxic effects. Secondly, we hoped to detect differences in the response of cancerous and noncancerous cells to the treatments. We choose MCF7 (breast carcinoma) and MCF10A (noncancerous immortalized breast epithelium) cells as a well-studied pair of cancer-control cell lines. The MCF7 cells are known to respond to bortezomib treatment, however they are relatively less sensitive than many other cancer cells (15, 16). We choose a peptide boronic acid derivative MG262 (carbobenzoxy-LeuLeuLeu-B(OH)₂; proteasome inhibitor III) and AAF-CMK as specific inhibitors of the proteasome and TPP II, respectively. MG262 is a close chemical homolog of bortezomib and both compounds block the chymotrypsin-like activity of the proteasome in a nearly identical manner (17). AAF-CMK competitively restrains the proteolytic activity of the TPP II *in vitro* and *in vivo* (12, 13). We found that cytotoxic effects of the two compounds were synergistic. Even more importantly, a combination of low doses of both inhibitors effectively killed the cancerous cells allowing the noncancerous cells to recover.

Materials and Methods

Cell culture and treatment with inhibitors.

MCF7 and MCF10A breast – derived cells were obtained from American Type Culture Collection (ATCC; Rockville, MD) and cultured according to the ATCC recommendations. The cells were cultured in 24-well plates to achieve initial confluence (time = 0 hours) of about 30%. The number of dead cells was determined with a trypan blue exclusion assay. The culture medium was removed from wells, the cells were overlaid with 0.1% solution of trypan blue in PBS, and the transparent (live) and blue (dead) cells were counted under inverted microscope (magnification 40x). The counts from 3 – 6 fields were averaged and standard deviations were calculated. The protease inhibitors: MG262 and AAF-CMK were obtained from Calbiochem and Sigma, respectively. Stock solutions of the inhibitors were prepared in dimethylsulfoxide (DMSO). The inhibitors were added at the time of cell plating in the amount of the solvent no larger than 1% of the total volume of the cell culture medium. Consequently, DMSO at final 1% concentration was also added to the control culture. The cells were counted after 12, 24, and 48

hours. To determine total DNA content and proteolytic activities (see below), the cells were cultured for 48 hours.

Fluorometric determination of total DNA content and proteolytic activities in cell lysates.

Propidium iodide (PI) was used to determine total content of DNA in the cells and fluorogenic peptide substrates, succinyl-LeuLeuValTyr-7-amino-4-methylcoumarin (SucLLVY-MCA) and AlaAlaPhe-7-amino-4-methylcoumarin (AAF-MCA), were used to determine peptidase activities of the proteasome and TPP II, respectively. To prepare total cell lysates the culture medium was removed, the cells in each well were overlaid with 200 μ L of water and then the cells were exposed to two cycles of freezing at -80°C for 3 hrs. and then thawing them at 37°C for 30 min. Propidium iodide was added to each well, mixed with the lysate, and the fluorescence was measured in the plates using a Kodak ImageStation 2000R with an emission filter at 600 nm. Alternatively, the protease substrates were added to final concentration 100 μ M in 20 mM Tris buffer, pH 7. After an incubation at 37°C for 1hr, fluorescence of MCA released from the substrates as a measure of peptidase activity was determined with an emission filter at 435 nm of a Fluoroskan Ascent plate reader (Thermo). Subsequently, the fluorescence intensity measured in arbitrary units was recalculated into the molar concentration on the basis of measurements of free MCA (Sigma) executed under the identical conditions. Finally, the peptidase activity was expressed as micromoles of MCA released from the corresponding substrate during its one hour incubation at 37°C per PI - determined cell count.

Statistical analysis of the data was accomplished using SPSS v.11 statistical package (SPSS Inc., Ill) with graphical support from SigmaPlot v.8 package (SYSTAT Software Inc., Cal.).

Results

AAF-CMK and MG262 used separately are cytotoxic for the cultured breast cells.

The cancerous and noncancerous breast cells were treated with varying concentrations of specific inhibitors of TPP II or the proteasome. All tested concentrations of both the compounds exhibited a detectable level of cytotoxicity toward both the cell lines (Figure 1). The effects of treatment with AAF-CMK, the specific inhibitor of TPP II, were similar for MCF7 and MCF10A cells when low, up to 5 μ M, concentrations of the compound were used. At higher concentrations, AAF-CMK was more toxic for the noncancerous MCF10A cells than for the MCF7 cells. To the contrary, the cancerous cells were always significantly more susceptible to cytotoxic effects of the proteasome inhibitor than noncancerous cells.

First, the cells were treated with AAF-CMK in a range of concentrations from 1 μ M to 50 μ M. The control cultures reached near-confluence after two days, with an almost identical total cell count for the MCF7 and MCF10A cell lines. After that time, less than 1% of total cell number in control populations were dead as detected with trypan blue stain. Lower concentrations of AAF-CMK exhibited moderate effect on survival of the cells and significant effect on their proliferation. After 48 hours of exposure to the lowest tested concentration of AAF-CMK (1 μ M), the count of viable MCF7 and MCF10A cells ranged between 65% and 69% of the control cell count, respectively, with only a few percent of dead cells (Figure 1A, B). Exposure to 5 μ M of the inhibitor, on the other hand, lowered the viable cell count to 35% and 38% of the control count, with 5% and 15% of dead cells (MCF7 and MCF10A, respectively). Effects of the treatment with 10 μ M AAF-CMK were similar to effects observed for 5 μ M AAF-CMK (Figure 1A, B). No statistically significant differences in proliferation (total cell count or

viable cell count) between the MCF7 and MCF10A were observed for the lower inhibitor concentrations, up to 20 μ M (Figure 1A). The percent of dead cells, however, was significantly higher ($P<0.01$) in MCF10A cells treated with 20 μ M or 50 μ M of AAF-CMK (Figure 1B). The difference was especially striking for the highest used concentration of the TPP II inhibitor. Under such conditions, 95% of the MCF10A cells were dead, as compared to only 31% of the MCF7 cells (Figure 1A, B).

The inhibitor of the proteasomal chymotrypsin-like activity, MG262, was used at concentrations ranging from 10 to 100 nM. The differences between MCF7 and MCF10A cells were statistically significant ($P<0.05$) for all used concentrations of the inhibitor and for both the viable cell count and the percent of dead cells (Figure 1C, D). As shown in Figure 1D, the percent of the dead cancerous MCF7 cells systematically increased with increasing concentrations of the MG262 inhibitor, reaching more than 60% after 48 hours of exposure to the highest used concentration compound (100 nM). The percent of dead noncancerous cells never reached 20 under the same conditions (Figure 1D). The count of live MCF7 cells after two-day treatment with the highest used concentration of MG262 (100 nM) reached only about 10% of the control cell count. However, the noncancerous cells were not refractory to the treatment, and their total count dropped to less than 40% of the control count with 50 nM or 100 nM MG262 present in the culture medium (Figure 1C). When the cells were counted after shorter exposure times (12 hours and 24 hours), the trends of increasing dead cell count and decreasing number of viable cells for different doses of the drugs remained the same as for the 48 hours exposure, but less pronounced (not shown). In general, none of the conditions used provided the desired effect of a high toxicity for the cancerous cells and a low toxicity for the control cells.

Combined treatment with AAF-CMK and MG262 results in a synergistic cytotoxic effect.

As the next step, we treated cells with twelve combinations of different concentrations of the inhibitors of TPPII and the proteasome. AAF-CMK at concentrations of 5, 10 and 20 μ M representing up to 50% of its observed efficacy for MCF10A cells was combined with 10, 20, 50 or 100 nM of MG262 for a 48-hours treatment. We excluded the highest (50 μ M) and the lowest (1 μ M) concentrations of AAF-CMK from the array of treatment conditions as, respectively, too toxic, especially for the control cells, and too mild (Figure 1B). As it can be seen in Figure 2, for all the conditions used the cytotoxic effect was stronger for the cancerous cells than for the noncancerous cells, with no more than 30% of the MCF7 cells surviving the treatment. For all but three conditions, the difference between viable cell counts for MCF7 and MCF10A was statistically significant ($P<0.05$ or better; see Figure 2 for details), with the counts of viable cancerous cells often falling to single-digits. The differences between the dead cell counts were less systematic. When the highest concentration of AAF-CMK (20 μ M) was combined with any MG262 dose, or when 10 μ M AAF-CMK was combined with 100 nM of MG262, more noncancerous than cancerous cells were still viable. However, a substantial number of dead noncancerous cells were observed under such conditions (Figure 2). This indicated that the MCF10A cells proliferated fast under the treatment (a high total cell count), but at least half of them quickly entered the apoptotic pathway (Figure 2). On the other hand, when 5 μ M (the lowest) dose of the TPP II inhibitor was used, the count of dead cells ranged between 4% and 7% of the total noncancerous cell count, and between 5% and 23% of the total cancerous cell count (Figure 2).

Table 1. The cytotoxic effect of the combined treatment with TPP II inhibitor and the proteasome inhibitor is synergistic for most doses of the compounds. The dead cell ratios represent % of dead cells as observed for a given combination of drugs divided by the % of dead cells as calculated assuming pure additivity of effects coming from both drugs. The higher the ratio, the stronger the synergy between drugs and the stronger cytotoxic effect against treated cells. The numbers in last column (the dead cells ratio for MCF7 divided by the dead cells ratio for MCF10A) indicate the particular conditions when synergistic cytotoxicity against the cancerous cells is relatively the strongest, as compared with the noncancerous cells.

AAF-CMK+MG262 [μ M] + [nM]	Dead cells ratio (combination/additive)		[ratio (MCF7)]/ [ratio (MCF10A)]
	MCF7	MCF10A	
5 + 10	1.7	4.0	0.43
5 + 20	2.7	3.3	0.81
5 + 50	3.3	1.2	2.60
5 + 100	5.3	1.0	5.20
10 + 10	1.5	6.7	0.23
10 + 20	2.4	3.1	0.77
10 + 50	3.9	1.6	2.40
10 + 100	4.0	4.5	0.89
20 + 10	2.5	7.3	0.34
20 + 20	3.7	7.9	0.47
20 + 50	3.9	2.6	1.50
20 + 100	2.7	2.1	1.30

To assess if the combined treatment produces a simple additive, antagonistic or synergistic effect, we calculated the “effect ratios” for cytotoxicity. We calculated ratios of the % of dead cells observed after treatment with the mixture of inhibitors to the geometric average of the sums of % of dead cells observed after the appropriate single-inhibitor treatments. The ratio equal or close to one indicated a simple additive effect of the two drugs. The ratio higher than one indicated synergistic effects of the treatment with the compounds in mixture, with highest ratios indicating strongest synergy and high cytotoxicity. The ratio lower than 1 would indicate an antagonistic effect. For the MCF7 cells the ratios were always higher than 1.5 (Table 1). For the MCF10A cells, the ratios suggested an additive effects in two cases (combinations: 5 μ M + 50 nM and 5 μ M + 100 nM, see Table 1), and synergistic in all others. Interestingly, the synergy effect with MCF10A was very high for selected combinations (10 μ M + 10 nM, 20 μ M + 10 nM and 20 μ M + 20 nM), pointing at these particular conditions as especially dangerous for noncancerous cells. When the cancerous MCF7 cells were analyzed, the ratios were highest (>3) for the following mixtures of inhibitors: 5 μ M + 100 nM (AAF-CMK + MG262), 10 μ M + 50 nM, 10 μ M + 100 nM, 20 μ M + 20 nM and 20 μ M + 50 nM (Table 1). To select the best conditions differentiating between MCF7 and MCF10A cells, we divided the appropriate ratios for MCF7 cells by the ratios calculated for MCF10A cells. The high “MCF7/MCF10A index” indicated that the particular conditions were significantly more toxic for the cancerous cells than the control cells. The indexes for three conditions clearly stood out: for 5 μ M + 50 nM, 5 μ M + 100 nM and 10 μ M + 50 nM (Table 1). The high indexes strongly suggested that the combined

treatment should better differentiate between the cancerous and noncancerous cells than single-drug treatment.

Table 2. The combined treatment with selected doses of the inhibitors is beneficial for selective targeting of cancerous MCF7 cells. The differences between the % of dead cells and % of viable cells are shown. The higher the differences, the better selectivity in targeting cancerous cells. The highest values of Δ_d and Δ_v are in **bold**. Note that one drug combination (10 μ M + 50 nM) produced high differences in both Δ_d and Δ_v categories.

Cells treated with:	Δ_d [% dead MCF7 - % dead MCF10A]	Δ_v [% viable MCF10A - % viable MCF7]
MG262 [nM]		
10	12	36
20	16	34
50	13	13
100	41	16
AAF-CMK+MG262 [mM] + [nM]		
5 + 10	-2	5
5 + 20	11	8
5 + 50	22	8
5 + 100	80	25
10 + 10	-8	5
10 + 20	18	26
10 + 50	43	33
10 + 100	22	12
20 + 10	-9	10
20 + 20	12	27
20 + 50	28	23
20 + 100	34	32

The combined treatment with the TPP II and the proteasome inhibitors better differentiated between the cancerous and noncancerous cells than a treatment with the proteasome inhibitor alone.

When the cells were treated with single inhibitors, the proteasome inhibitor was significantly more toxic for the cancerous than for the control cells (Figure 1). The effects of treatment with the TPP II inhibitor were less desirable: either no difference between the cell lines or higher toxicity against the noncancerous cells (Figure 1). To verify the usefulness of the combined treatment and to find the best conditions, we compared differences between the percent of dead cells for the two cell lines treated with the proteasome inhibitor only or with a combination of drugs. As can be seen in Table 2, in two cases of the combined treatment the differences between MCF7 and MCF10A cells were higher than the highest difference observed with the single inhibitor. Not surprisingly, these conditions: 5 μ M + 100 nM and 10 μ M + 50 nM (AAF-CMK + MG262), were also found to produce strong synergistic cytotoxic effects against MCF7 cells (Table 1). To pay attention not only to cytotoxicity against the cancerous cells but also to

survival of the noncancerous cells, we also compared differences between the percent of viable cells for the two cell lines. Two lowest doses of the proteasome inhibitor and two mixtures of the compounds: 10 μ M + 50 nM and 20 μ M + 100 nM, caused nearly the same, high differences, favoring survival of the noncancerous cells (Table 2). Interestingly, one of the combinations, 10 μ M of AAF-CMK + 50 nM of MG262 was always among the best conditions, whether the synergistic effects were analyzed or the advantage over the treatment with the proteasome inhibitor was assessed (Tables 1, 2). Indeed, the effects of the treatment with the 10 μ M + 50 nM mixture seemed to be relatively mild for the noncancerous cells: 40% of the cells were still viable after the 48 hours of culture. Only 6% of MCF7 cells remained viable after such treatment (Figure 2). The 10 μ M + 50 nM combination of AAF-CMK and MG262 was selected for further analysis.

Discussion

The involvement of ubiquitin-proteasome system in cancerogenesis and the usefulness of the proteasome as anti-cancer drug target are now fully established (2, 9). Bortezomib, the inhibitor of the proteasome, proved to be a very efficient drug in multiple myeloma treatment and at least a promising compound for treatment of other cancers (10). To improve actions of bortezomib, combinations of the inhibitor with drugs inducing apoptosis have been tested and many of them have shown synergistic effects. The notable examples of drugs synergizing with the proteasome inhibitor are gemcitabine and TRAIL (tumor necrosis factor-related apoptosis-inducing ligand) (18, 19). The common notion of the compounds tested in combination with bortezomib is that these are drugs already used for chemotherapy, and that bortezomib often abolishes resistance of cancer cells for these drugs. The distinct approach we took in this study called for a combination of the proteasome inhibitor with a compound not known for its specific anti-cancer potency. Instead, we assumed that targeting controlled proteolysis downstream from the proteasome may enhance the anti-cancer actions of the proteasome inhibitor. TPP II is known to process products of proteasomal degradation (7). The specific inhibitor of TPP II, AAF-CMK at 5 μ M or 10 μ M, did not show significant effects on proliferation of mouse lymphoma EL4 cells in previous studies (12, 13). To the contrary, breast cell lines analyzed here were sensitive to the treatment with AAF-CMK at all concentrations tested, from 1 μ M to 50 μ M. The discrepancy may originate in distinct physiological characteristics of the lymphoma and breast cell lines used. Notably, the cytotoxic effect of AAF-CMK was more pronounced with the noncancerous than with cancerous breast cells. The physiological roles of TPP II in the two cell lines have not been tested, however we observed that cytosolic fractions prepared from MCF10A cells consistently exhibited up to a 10-fold higher activity of TPP II than cytosols from MCF7 cells (Osmulski and Gaczynska, unpublished observations). This significant difference in activity may indicate distinct functions of TPP II in cancerous and noncancerous cells, a notion worth to explore. So far, TPP II has been found up regulated in Burkitt's lymphoma B-cell tumor (20). Treatment with 10 μ M or 15 μ M of AAF-CMK caused apoptosis in these cells but not in the cells with several-fold lower levels of expression and activity of TPP II (20). These results are in full agreement with our observation that cells with higher activity of TPP II were more sensitive to treatment with AAF-CMK. Interestingly, general resistance to apoptosis was observed in human embryonic kidney 293 cells with overexpressed TPP II (21) and in mouse lymphoma cells with high TPP II activity (22).

The cytotoxic effects of MG262, a close homolog of bortezomib, were predictably more pronounced for the MCF7 than for MCF10A cells (23). The origin of generally distinct response of cancerous and noncancerous cells to proteasome inhibitors is not clear. Significant differences in the subunit composition of the proteasomes in MCF7 than on MCF10A cells have been reported (24), however many other elements of cellular physiology most likely also contribute to the distinct reaction to proteasome inhibition. It is essential to emphasize though that the MCF10A noncancerous cells were not refractory to the treatment with the proteasome inhibitor, which exemplifies the limitations of chemotherapy with the proteasome inhibitor alone. Interestingly, the activity of the proteasome in cytosolic fraction of the MCF7 cells appeared to be about two-fold higher than in the MCF10A cells (Osmulski and Gaczynska, unpublished observations). The activity was assessed with a model peptide substrate specific for the chymotrypsin-like proteasomal active site, considered the most important and targeted by MG262 and by bortezomib. This observation suggests an interesting possibility of a rule common for both the proteasome and TPP II that the cytotoxic effect of an inhibitor is stronger in cells with higher activity of the targeted protease. Nevertheless, the results of treatments with the proteasome and the TPP II inhibitors alone showed at the best moderately selective targeting of the cancerous MCF7 cells.

Treatment of cells with combinations of the proteasome and TPP II inhibitors revealed a high toxicity against the cancerous cells and significantly milder effects on the noncancerous cells. For most concentrations of the inhibitors used the effects were synergistic for both cell lines. Fortunately, for MCF10A cells several conditions showed additive or only mildly synergistic cytotoxic actions. Even more importantly, the same additive conditions exhibited a high level of synergy when the MCF7 cells were treated. For the best combination found, the percentages of viable and dead noncancerous cells were nearly identical with the results for a single-inhibitor treatment with the respective concentration of AAF-CMK alone. To the contrary, the effect of this combination of inhibitors on the cancerous cells was much more severe than any of the respective single-inhibitor treatments. It seems that combined treatment alleviated the cytotoxic effects of the proteasome inhibitor only on noncancerous cells but not on cancerous cells. The reason of such distinct responses of both cell lines is unknown. Perhaps such a desired reaction to these inhibitors will be limited to noncancerous cells with relatively low activity of the proteasome and high activity of TPP II, and cancerous cells displaying just opposite profile of activities of collaborating proteases. It would be also interesting to test the response of cells with high activities of both the proteasome and TPP II to the inhibitor treatment. Skeletal muscle during sepsis are example of such profile of activities (25, 26). Additional experiments involving other cell lines and analyzing of the inhibitor-induced changes in the ubiquitin-proteasome pathway will be necessary to understand at least some aspects of the detected differences in cytotoxicity levels. Nevertheless, our results clearly show beneficial effects of simultaneous targeting of the proteasome and a downstream protease in differentiating between the studied cancerous and noncancerous breast cells.

Literature

1. Varshavsky, A. Regulated protein degradation, *Trends in Biochemical Sciences*. 30: 283-286, 2005.
2. Mani, A. and Gelmann, E. P. The ubiquitin-proteasome pathway and its role in cancer, *Journal of Clinical Oncology*. 23: 4776-89, 2005.

3. Orlowski, R. Z. and Baldwin, A. S. NF-kappa B as a therapeutic target in cancer, *Trends in Molecular Medicine.* 8: 385-389, 2002.
4. Ikeda, K. and Inoue, S. Estrogen receptors and their downstream targets in cancer, *Archives of Histology & Cytology.* 67: 435-42, 2004.
5. Ohta, T. and Fukuda, M. Ubiquitin and breast cancer, *Oncogene.* 23: 2079-88, 2004.
6. Hendil, K. B. and Hartmann-Petersen, R. Proteasomes: a complex story, *Current Protein & Peptide Science.* 5: 135-51, 2004.
7. Reits, E., Neijssen, J., Herbergs, C., Benckhuijsen, W., Janssen, L., Drijfhout, J. W., and Neefjes, J. A major role for TPPII in trimming proteasomal degradation products for MHC class I antigen presentation., *Immunity.* 20: 495-506, 2004.
8. Tomkinson, B. and Lindas, A. C. Tripeptidyl-peptidase II: A multi-purpose peptidase., *The International Journal of Biochemistry and Cell Biology.* 37: 1933-1937, 2005.
9. Orlowski, R. Z. and Dees, E. C. The role of the ubiquitination-proteasome pathway in breast cancer: applying drugs that affect the ubiquitin-proteasome pathway to the therapy of breast cancer, *Breast Cancer Research.* 5: 1-7, 2003.
10. Rajkumar, S. V., Richardson, P. G., Hideshima, T., and Anderson, K. C. Proteasome inhibition as a novel therapeutic target in human cancer, *Journal of Clinical Oncology.* 23: 630-9, 2005.
11. Geier, E., Pfeifer, G., Wilm, M., Lucchiari-Hartz, M., Baumeister, W., Eichmann, K., and Niedermann, G. A giant protease with potential to substitute for some functions of the proteasome, *Science.* 283: 978-81, 1999.
12. Glas, R., Bogyo, M., McMaster, J. S., Gaczynska, M., and Ploegh, H. L. A proteolytic system that compensates for loss of proteasome function, *Nature.* 392: 618-622, 1998.
13. Princiotta, M. F., Schubert, U., Chen, W. S., Bennink, J. R., Myung, J., Crews, C. M., and Yewdell, J. W. Cells adapted to the proteasome inhibitor 4-hydroxy5-iodo-3-nitrophenylacetyl-Leu-Leu-leucinal-vinyl sulfone require enzymatically active proteasomes for continued survival, *Proceedings of the National Academy of Sciences of the United States of America.* 98: 513-518, 2001.
14. Wang, E. W., Kessler, B. M., Borodovsky, A., Cravatt, B. F., Bogyo, M., Ploegh, H. L., and Glas, R. Integration of the ubiquitin-proteasome pathway with a cytosolic oligopeptidase activity, *Proceedings of the National Academy of Sciences of the United States of America.* 97: 9990-5, 2000.
15. An, W. G., Hwang, S. G., Trepel, J. B., and Blagosklonny, M. V. Protease inhibitor-induced apoptosis: accumulation of wt p53, p21WAF1/CIP1, and induction of apoptosis are independent markers of proteasome inhibition, *Leukemia.* 14: 1276-83, 2000.
16. Teicher, B. A., Ara, G., Herbst, R., Palombella, V. J., and Adams, J. The proteasome inhibitor PS-341 in cancer therapy, *Clinical Cancer Research.* 5: 2638-2645, 1999.
17. Gaczynska, M. and Osmulski, P. A. Small-molecule inhibitors of proteasome activity, *Methods in Molecular Biology.* 301: 3-22, 2005.
18. Kamat, A. M., Karashima, T., Davis, D. W., Lashinger, L., Bar-Eli, M., Millikan, R., Shen, Y., Dinney, C. P., and McConkey, D. J. The proteasome inhibitor bortezomib synergizes with gemcitabine to block the growth of human 253JB-V bladder tumors in vivo, *Molecular Cancer Therapeutics.* 3: 279-90, 2004.
19. Lashinger, L. M., Zhu, K., Williams, S. A., Shrader, M., Dinney, C. P., and McConkey, D. J. Bortezomib abolishes tumor necrosis factor-related apoptosis-inducing ligand

resistance via a p21-dependent mechanism in human bladder and prostate cancer cells, *Cancer Research*. 65: 4902-8, 2005.

- 20. Gavioli, R., Frisan, T., Vertuani, S., Bornkamm, G. W., and Masucci, M. G. c-myc overexpression activates alternative pathways for intracellular proteolysis in lymphoma cells, *Nature Cell Biology*. 3: 283-8, 2001.
- 21. Stavropoulou, V., Xie, J., Henriksson, M., Tomkinson, B., Imreh, S., and Masucci, M. G. Mitotic infidelity and centrosome duplication errors in cells overexpressing tripeptidyl-peptidase II, *Cancer Research*. 65: 1361-8, 2005.
- 22. Hong, X., Lei, L., and Glas, R. Tumors acquire inhibitor of apoptosis protein (IAP)-mediated apoptosis resistance through altered specificity of cytosolic proteolysis, *Journal of Experimental Medicine*. 197: 1731-43, 2003.
- 23. Adams, J. Development of the proteasome inhibitor PS-341, *Oncologist*. 7: 9-16, 2002.
- 24. Johnsen, A., France, J., Sy, M. S., and Harding, C. V. Down-regulation of the transporter for antigen presentation, proteasome subunits, and class I major histocompatibility complex in tumor cell lines, *Cancer Research*. 58: 3660-7, 1998.
- 25. Hasselgren, P. O., Wray, C., and Mammen, J. Molecular regulation of muscle cachexia: it may be more than the proteasome, *Biochemical & Biophysical Research Communications*. 290: 1-10, 2002.
- 26. Wray, C. J., Tomkinson, B., Robb, B. W., and Hasselgren, P. O. Tripeptidyl-peptidase II expression and activity are increased in skeletal muscle during sepsis, *Biochemical & Biophysical Research Communications*. 296: 41-7, 2002.

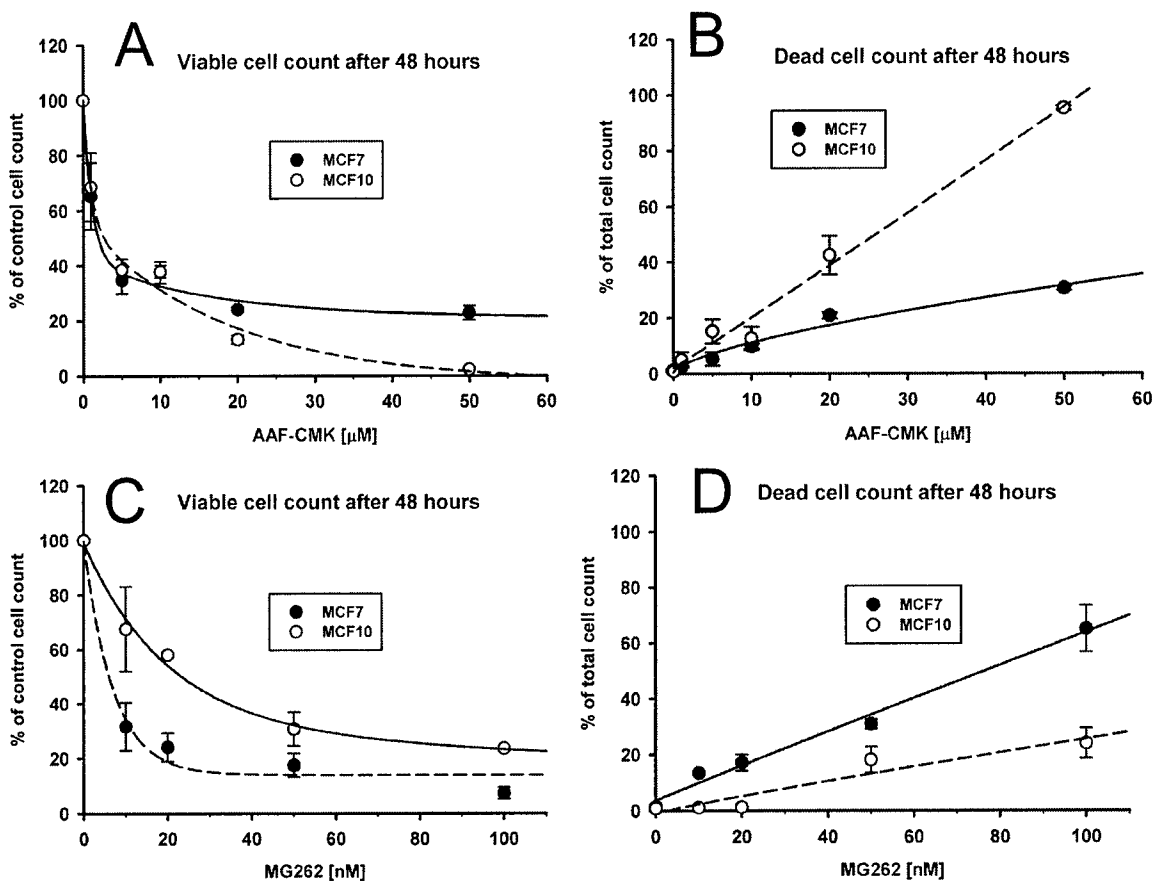


Figure 1. Inhibitors of TPP II (AAF-CMK) and the proteasome (MG262) were cytotoxic for MCF7 and MCF10A breast cells. The cells were cultured in the presence of indicated concentrations of AAF-CMK (A, B) or MG262 (C, D) for 48 hours. The viable and dead cells were distinguished by trypan blue exclusion assay and counted. The graphs represent relative content of viable cells (A, C) or of dead cells (B, D) calculated as percent of control viable cells and total control cells, respectively. The total count of control cells (no inhibitors) of both lines differed by less than 10%. Only $1.4\% \pm 0.3\%$ of MCF7 cells and $0.9\% \pm 0.3\%$ of MCF10A cells were classified as dead. The results represent averages from 3 – 6 fields of counted cells \pm standard deviations (SD). All differences between MCF7 and MCF10A cells treated with a given dose of MG262 are statistically significant (T test, $P < 0.05$). The differences between cancerous and noncancerous cells treated with AAF-CMK are significant for higher doses of the inhibitor (20 μ M and 50 μ M) and for percent of dead cells after treatment with 5 μ M of the drug.

Total cell count after 48 hours

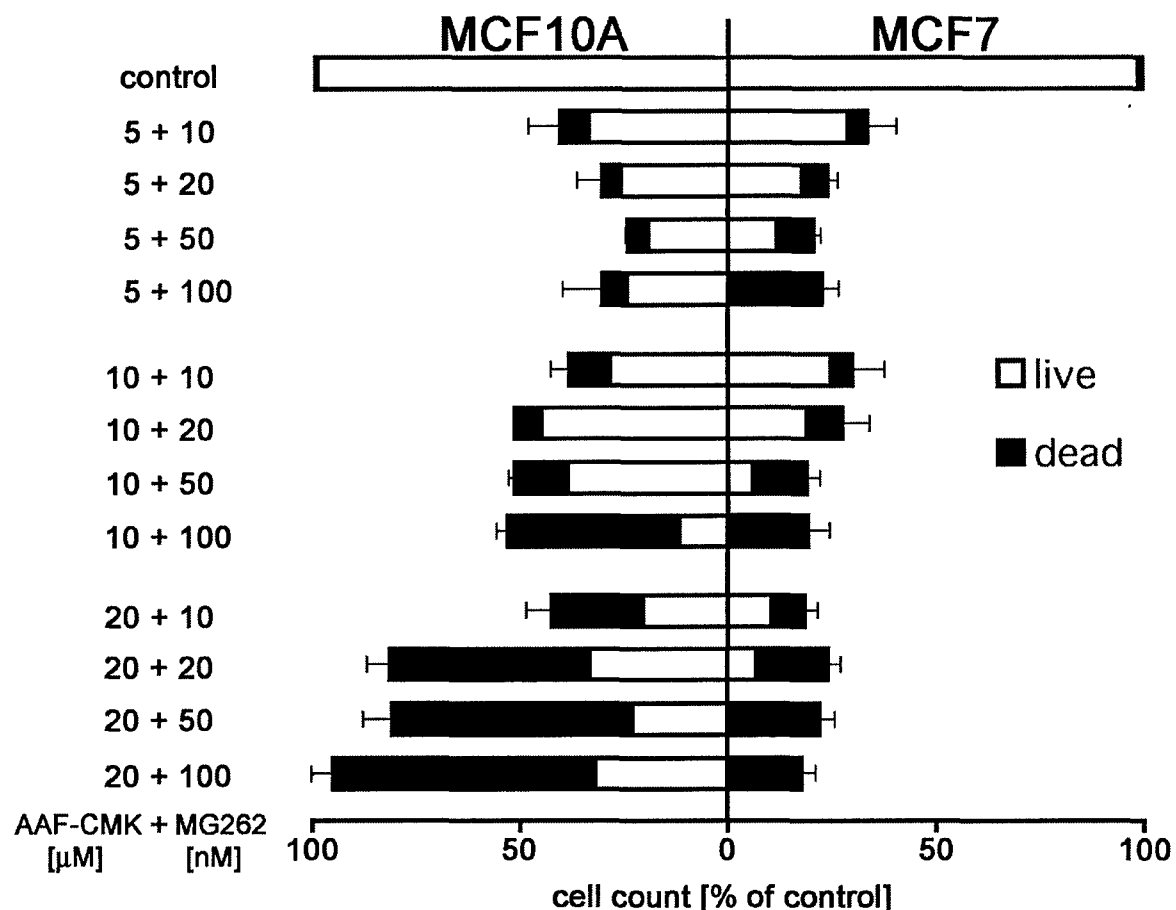


Figure 2. Treatment with combinations of AAF-CMK and MG262 was toxic for both MCF7 and MCF10A cells, however the noncancerous cells were generally less sensitive to drugs-induced inhibition of proliferation and induction of cell death than the cancerous cells. The cells were cultured for 48 hours in the presence of indicated doses of the inhibitors and counted as in Figure 1. Total height of the bars represents the total cell count as percent of the control (no inhibitors) count. The relative contributions of dead and viable cells in the total count are indicated by black and white colors, respectively. As in Figure 1, average counts from 3 – 6 fields are plotted. Standard deviations are shown for the total cell counts. The differences between percentages of viable MCF7 and MCF10A cells were statistically significant (T test, $P < 0.05$) for all conditions except (5+10), (5+20) and (10+10).

APPENDIX 2

Distinct subcellular localization of tripeptidyl peptidase II in breast cancer cells, as compared to noncancerous cells.

Pawel A. Osmulski, Elzbieta Jankowska, and Maria E. Gaczynska

Contribution from:

Institute of Biotechnology, Department of Molecular Medicine, University of Texas Health Science Center at San Antonio

15355 Lambda Drive, San Antonio, TX 78245

contact:

e-mail: Gaczynska@uthscsa.edu, phones: office (210) 567-7262 laboratory (210) 567-7259, (210) 567-7265, fax (210) 567-7269

Abstract

Tripeptidyl peptidase II (TPP II) is a large serine peptidase of subtilisin family present in almost all Eukaryotes. Its function in cellular protein turnover is not clear. It is suspected that it may participate in trimming products released by proteasome to prepare peptides for MHC class I presentation. Here we show that TPPII isolated from human breast cancer MCF7 and normal MCF10A cells forms a distinct pattern of posttranslationally modified bands representing a large molecular weight complex of TPPII. Four groups of bands were detected: 150, 165, 170, and 240kDa. The identified pattern of bands was specific for the cell line and a cell cycle stage. We also analyzed subcellular localization of the protease using AAF-CMAC substrate. We found presence of TPPII also in the nuclear fraction (in nuclear envelope) in the mitotic normal but not cancerous cells. We confirmed previous observation of the membrane localization of TPPII. Additionally, we noticed several fold higher peptidase activity in cytoplasm of the MCF10A cells. Possible consequences of the distinct localization and structural properties of TPPII in the cancerous cells is discussed.

Introduction.

Tripeptidyl peptidase II (TPP II, EC 3.4.14.10) is a ubiquitous eukaryotic serine protease of broad substrate specificity capable to sequentially remove tripeptides from N-termini of polypeptides and displaying a low endopeptidase activity (1). The enzyme is found mostly in the cytosol where it is known to take part in the ubiquitin-proteasome pathway of controlled proteolysis. Namely, TPP II acts downstream from the proteasome, trimming at least some products of the proteasomal degradation to the size preferred by the major histocompatibility complex (MHC) class I presentation machinery (2, 3). TPP II was also found on the extracellular side of membranes and the membrane-related variant cleaves and inactivates cholecystokinin (4). The distinctive feature of TPP II is its size: the 138 kDa subunits of the enzyme form giant homooligomers of about 4 MDa in the form of twisted rods, most likely self-compartmentalizing (1, 5). The full complex is necessary for the maximal enzymatic activity, however smaller assemblies display a limited tripeptidyl peptidase activity and the oligomerization was proposed as the major mechanism of regulation of actions of TPP II (6). A splicing variant of the subunit, with 13 additional amino acids, is capable to form even larger active assemblies (6).

The physiological role of TPP II is far from clear and most likely include more tasks than trimming selected MHC class I epitopes or inactivation of cholecystokinin. The application as a protease processing proteasomal products may be critical for efficient functioning of the ubiquitin-proteasome degradative pathway and recycling of amino acids. The increase of expression and activity of TPP II in skeletal muscle during sepsis strongly suggests such function (7). On the other hand, Burkitt's lymphoma cells with functional knockdown of TPP II were unable to complete mitosis, whereas overexpression of the TPP II in human embryonic kidney 293 cells correlated with mitotic infidelity and resistance to apoptosis (8). A more detailed picture of the role of TPP II in cell cycle, apoptosis and genetic instability, however, is missing. Here we demonstrate that TPP II changes its oligomerization status and subcellular distribution depending on the stage of cell culture. Moreover, we demonstrate that distinct oligomeric forms are built from phosphorylated or nonphosphorylated subunits, and that activity and oligomerization of TPP II differ in cancerous breast MCF7 cells and in non tumorigenic breast MCF10A cells.

Materials and Methods

Cell culture and cell extracts.

MCF7 (pleural effusion adenocarcinoma) and MCF10A epithelial breast – derived cells were obtained from American Type Culture Collection (ATCC; Rockville, MD) and cultured according to the ATCC recommendations in ... flasks. The cells were harvested on three stages of cell culture/cell cycle: (a) as nonsynchronized, nonconfluent at about 80% confluence; (b) as overconfluent harvested 6 hours after achieving 100% confluence; (c) arrested in metaphase by treatment with 15 micrograms/ml of nocodazole for 15 hours (9). For the purpose of microscopic observation of synchronized cultures, the cells were released from the arrest by replacing the nocodazole – containing medium with a fresh drug-free medium. The cells were trypsinized, pelleted and washed twice in phosphate-buffered saline (PBS). The cell pellet was fractionated into cytosolic, nuclear and membrane fractions by a following procedure. The cells suspended in homogenization buffer (10 mM Hepes pH 6.2, 10 mM NaCl, 1.5 mM MgCl₂) were broken by 80 strokes of a Dounce homogenizer. The pellet obtained after centrifugation of the lysate (3 min, 2,500xg, with additional washing of the pellet) was resolubilized in extraction buffer (10 mM Tris, pH 7.4, 10 mM NaCl, 5 mM MgCl₂, 1 mM dithiothreitol, 0.5% IgepalCA-630) and constituted the nuclear fraction. The supernatant was subjected to 1.5 – hour ultracentrifugation at 100,000xg. The resulting supernatant after the ultracentrifugation was saved as the cytosolic fraction. The remaining pellet after the solubilization in the extraction buffer yielded the membrane fraction. All procedures were carried out at 4°C, and all buffers were supplemented with a protease inhibitors and phosphatase inhibitors cocktail: 1 mM phenylmethylsulfonyl fluoride (PMSF), aprotinin, leupeptin, pepstatin (all at 1 µg/ml), 1 mM NaF and 1 mM NaVO₄.

Protein electrophoresis and Western Blotting.

The cytosolic, nuclear and membrane extracts or the purified TPP II were separated by SDS-PAGE (sodium dodecyl sulfate polyacrylamide gel electrophoresis), with 8% or 6% of acrylamide. Twenty µg of extract protein was loaded per well of mini gels. The proteins were Western blotted into nitrocellulose membrane and probed with specific polyclonal antibodies against fission yeast TPP II (rabbit; Alpha Diagnostics, San Antonio, TX). The blots were

developed with Lumi-Light Western Blotting substrate (Roche) and the bands were visualized with Kodak ImageStation 2000R.

Detection of activity of TPP II in living cells.

The MCF7 and MCF10A cells were grown on coverslips. The coverslips with nonsynchronized, nonconfluent, overconfluent or nocodazole-arrested cells were prepared. For visualization of the TPP II activity, the coverslips were wet-mounted on microscope slides with 10 microliters of PBS (phosphate-buffered saline) containing 500 micromolar model substrate AlaAlaPhe-7-amino-4-chloromethylcoumarin (AAF-CMAC). The AAF-CMAC was chosen as a substrate instead of the commonly used AlaAlaPhe-7-amino-4-methylcoumarin (AAF-MCA) fluorogenic peptide (7), because of the lower intracellular diffusion rates of the CMAC fluorescent group than the MCA group (Molecular Probes Handbook). The AAF-CMAC is not commercially available and was synthesized as outlined below. Propidium iodide (PI) at the final concentration of 0.3 mg/ml was added to PBS to visualize dead cells easily permeable for PI. After 10 min. of preincubation at room temperature, the slides were analyzed under the fluorescent microscope (Zeiss AxioVision 2) with the excitation/emission filter used for DAPI visualization. The presence of propidium iodide bound to DNA was detected with the Texas Red filter of the microscope. To visualize DNA in the cells together with the TPP II activity, the coverslips with cells after at least 20 min incubation with AAF-CMAC were briefly washed with cold 50% ethanol, dried in air and wet-mounted on slides with PBS containing 0.3 mg/ml of PI.

Synthesis of AAF-CMAC.

Amino acids and peptide synthesis reagents were purchased from Advanced ChemTech or from Sigma/Aldrich. Solvents were obtained from Fisher and Fluka. CMAC was purchased from Molecular Probes. All products were analyzed using reverse-phase high performance liquid chromatography (RP-HPLC), column: XTerra RP C₁₈, 5 μm, 4.6 x 250 mm (Waters), developed with a gradient from 0 to 100% B, 30 min., where A: water + 0.1% trifluoroacetic acid (TFA), B: 80% acetonitrile/water + 0.1% TFA. A Delta 600E HPLC system from Waters was used to run and analyze chromatograms. The synthesis of H-AAF-OH was carried out on Advanced ChemTech Model 90 Peptide Synthesizer using Fmoc-strategy and preloaded Wang resin (Fmoc-Phe-Wang resin, 0.8 mmol/g). As the next step, -Butyloxycarbonyl (Boc) protecting group was coupled to the N-terminus of the peptide using the standard procedure described in the literature (Tarbell et al., 1971). The solution of the peptide in a mixture of 1,4-dioxane, water and 1 M NaOH was stirred and cooled in an ice/water bath. Di-tert-butylpyrrocarbonate was added in portions, pH adjusted to 8-9, and stirring continued overnight at the room temperature. The solution was concentrated *in vacuo*, cooled in an ice/water bath, covered with a layer of ethyl acetate and acidified with 1 M potassium hydrogensulfate to pH 2-3. The aqueous phase was extracted with ethyl acetate. The organic extracts were pooled, washed with water, dried over anhydrous magnesium sulfate and evaporated *in vacuo*. The residue was purified using RP-HPLC (XTerra Prep MS C₁₈ column, 5 μm, 19 x 50 mm). The pure product (10.2 mg) was obtained. R_T = 25.69 min. Incorporation of CMAC moiety to obtain Boc-AAF-CMAC was done by the mixed anhydride procedure (Meienhofer J., 1979). Boc-AAF-OH was dissolved in anhydrous tetrahydrofuran (THF) and cooled to -15°C (ice/ethanol). N-methylmorpholine was added followed by isobutyl chloroformate. The mixture was allowed to react in -15°C for 15 min. to form a mixed anhydride. The solution of 7-amino-4-chloromethylcoumarin (CMAC) in anhydrous THF was added and the reaction mixture left stirring for 1 hour at -15°C and

additional 2 hours at the room temperature. The crude product was purified using RP-HPLC. 5.76 mg of the pure product was obtained. $R_T = 29.16$ min. Boc group was removed using 50% TFA/dichloromethane solution. The product was lyophilized giving 4.8 mg of foam. $R_T = 22.11$ min. MS: 499.15, calc. $M = 498.96$ Da. For biological studies, the probe was dissolved at concentration 10mM in DMSO (stock solution) and kept at -80°C . Directly before its use, AAF-CMAC was further diluted to 1mM with DMSO. The probe shows absorption maximum at 354 nm and emission at 464 nm.

Results.

The pattern of TPP II subunits differed between the MCF7 and MCF10A cell lines, between their subcellular fractions and between extracts from cells in distinct physiological state.

Western blotting of cellular extracts with specific anti - TPP II antibodies recognized four bands of apparent molecular weights of about 150 kDa, 165 kDa, 170 kDa and 240 kDa. Interestingly, the TPP II was present not only in the cytosolic fraction, but also in membrane, and under specific conditions, in the nuclear fraction. As can be seen in Figure 1, distinct subcellular fractions consistently displayed distinct pattern of subunits, summarized in Table 1.

Table 1 The pattern of TPP II subunits detected by Western blotting in subcellular compartments of cancerous and control breast cells (see Figure 1).

Culture conditions	Cellular fraction	MCF7 (kDa)	MCF10A (kDa)
not synchronized	Cytosolic	240, 165	170, 165
	Membrane	165	170, closely spaced doublet
	Nuclear	not detectable	traces of 170 kDa band
overconfluent (G_0)	Cytosolic	240, 170, 150	240, 170
	Membrane	165, 150	170, 165
	Nuclear	not detectable	not detectable
mitotic	Cytosolic	240, 165	240, 170
	Membrane	165	170, closely spaced doublet
	Nuclear	not detectable	170

Figure 1 shows that the 170 kDa band was the most commonly present in MCF10A cells, especially in cytosolic fraction, and the 165 kDa band seemed to replace the 170 kDa subunit in MCF7 cell extracts. The 240 kDa subunit, on the other hand, was always present in cytosols of both cell lines. The band of lowest apparent molecular weight, 150 kDa, was detected only in membranes and cytosol of overconfluent MCF7 cells. The most striking feature, however, was the presence of a prominent 170 kDa band in the nuclear extracts of MCF10A cells arrested in a metaphase. Traces of the protein were detected in nuclear extracts from not synchronized MCF10A, a result consistent with a prediction that a small portion of such the cells was in metaphase at the time of cell breaking and extract preparation.

The presence of TPP II in nuclear extract was the most prominent difference observed between the cancerous and noncancerous breast cells. The other differences included a strong 165 kDa band in the membrane fraction isolated from overconfluent MCF7 cells. Interestingly, the overall pattern of detected subunits was very similar in all the extracts of nonsynchronous and mitotic MCF7 cells, but not MCF10A cells.

Subcellular distribution of TPP II activity differs between MCF7 and MCF10A cells.

Degradation of the fluorogenic substrate AAF-CMAC by the TPP II was first assessed *in vitro* with purified samples of the protease. Then, the conditions were established to observe the activity *in vivo*, in MCF10A and MCF7 cells growing on coverslips and incubated with the substrate while wet-mounted on microscope slides. The concentration of the substrate and preincubation time used were sufficient for apparent saturation of the degradation reaction, since adding more of the AAF-CMAC or increasing preincubation time did not significantly change the observed intensity of the reaction. The fluorescence of fixed cells was stable for at least an hour of observation and no significant diffusion of the CMAC was observed.

Apparently, the incubation with AAF-CMAC did not induce apoptosis or otherwise harm the cells since we routinely observed no more than 5% of PI-permeable cells in the unfixed populations of MCF10A and MCF7 cells. The images of MCF10A and MCF7 cells shown in Figures 2-5 have been brought to similar brightness by image processing software (Adobe Photoshop 5.5) for clarity and convenience of presentation. However, the overall intensity of fluorescence of CMAC in nonsynchronous MCF10A cells was significantly higher than the corresponding fluorescence in nonsynchronous MCF7 cells and consistently required 5 to 10-fold shorter exposure times for the comparable image quality. The images of living cells degrading the fluorescent substrate of the TPP II clearly showed the subcellular localization of the protease: cytosol, together with membrane structures, and nuclear envelope (Figure 2). Consistently with the above Western blotting results, we detected changes in subcellular localization of the TPP II activity during the progression through the cell cycle when imaging nonsynchronous cells, cells arrested on the onset of mitosis with nocodazole, cells released from the nocodazole arrest, and overconfluent cells. Importantly, we were able to precisely follow the changes in both types of cells, especially the emergence and dispersion of the activity localized in and around a nuclear envelope.

As can be seen in Figures 2 - 4, the CMAC – releasing activity was always present in the cytosol, albeit it was faint in overconfluent (G_0) cells. With the exception of G_0 cells (Figure 3), a strong CMAC fluorescence were detectable in the nucleus when the nuclear membrane was still present. A very strong fluorescence around/in the nuclear envelope appeared in late G2 and/or on the onset of mitosis and persisted until the nuclear membrane disappeared (Figure 2, 4). For a brief period during chromatin condensation a very strong fluorescence colocalized with the emerging chromosomes. Subsequently, on late stages of the condensation of chromatin, the fluorescence diffused into the cytosol leaving only a faint border around condensed chromosomes (Figure 4). We observed the following differences between the intensity and distribution of CMAC fluorescence in MCF10A and MCF7 cells. First, the fluorescence around nuclear envelope appeared stronger in relation to the cytoplasmic background in nonsynchronous MCF7 than in MCF10A cell (Figure 2). Second, the strong fluorescence around nuclear envelope appeared already in G2 in MCF7 cells, whereas it correlated rather with the onset of mitosis in MCF10A cells. There were many more cells with well-visible fluorescence around nuclear envelope in nonsynchronous population of MCF7 cells, than in MCF10A cells (Figure 2).

Discussion

Tripeptidyl peptidase II was known so far as a cytosolic enzyme with a membrane – embedded variant, built from multiple subunits of molecular weight of about 138 kDa (1). In this study we show a much more complicated picture: subunits of multiple apparent molecular weights and of dynamic cytosolic, membrane or nuclear envelope localizations. Moreover, the pattern of subunits and their localization significantly differed between the two breast cell lines, the cancerous MCF7 and noncancerous MCF10A. The presence of subunits in the range of several apparent molecular weights suggests posttranslational modifications, since the reported before splicing variant of the subunit differs only by 13 amino acids, much too little to produce a detectable shift during SDS-PAGE (6). Indeed our preliminary data strongly suggest that all the TPP II subunits except the 150 kDa band are phosphorylated. Distinct patterns of phosphorylation may provide means for precise regulation of activity and oligomerization (Osmulski and Gaczynska, submitted), and perhaps also subcellular localization. It is possible that majority of TPP II subunits present in the cell are modified, henceforth the lack of a 138 kDa band in our Western blots. The 150 kDa version may be modified in a distinct manner or, most probably, their phosphorylation may have not been detectable by the antibodies used. Analysis of phosphorylation sites by mass spectroscopy is currently in progress and will address this problem.

Our Western blotting data were fully confirmed by detection of the TPP II activity in living cells with the specific fluorogenic peptide substrate. We were able to confirm the localization of TPP II in nuclear fraction, apparently in the nuclear envelope region and chromatin. The activity of “nuclear” TPP II indeed appeared significantly lower in MCF7 than in MCF10A cells, which explains the lack of detectable TPP II bands in nuclear extracts of cancerous cells.

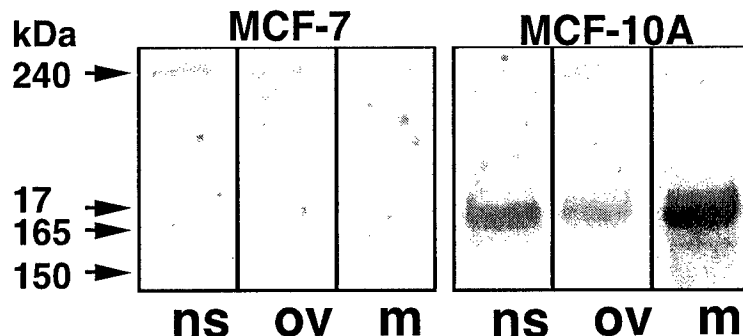
Based on the Western blotting and intracellular activity data, we propose the following model of localization of TPP II. In the case of the MCF10A cells the most of the TPP II resides in the cytosol as the large form built from 170 kDa phosphorylated polypeptide with a presumably over phosphorylated minor component of 240 kDa. A small portion of the TPP II is also bound to ER membranes and perhaps cell membrane mostly as 170 kDa doublet and 165 kDa phosphopolypeptide. The biochemical basis for the formation of the 170 kDa doublet remains at this moment unknown. The membrane-localized TPP II probably plays a distinct role from the cytosol-confined protease since it is specifically localized to this compartment in the overconfluent cells. At a certain point before metaphase the TPP II enters the nuclear envelope region and then remains there for the most of this stage. The total amount of the TPP II increases during mitosis followed by the increase of its phosphorylation. Upon the completion of the mitosis the TPP II is probably destroyed by unknown pathway with the possible signaling through overphosphorylation.

The striking differences between MCF7 and MCF10A cells remain unexplained, however they provide perfect starting point for further studies on the possible role of TPP II in cell cycle regulation.

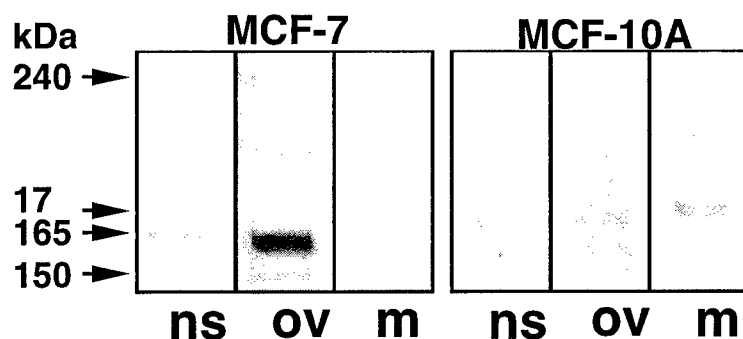
LITERATURE

1. Tomkinson, B. and Lindas, A. C. Tripeptidyl-peptidase II: A multi-purpose peptidase., The International Journal of Biochemistry and Cell Biology. 37: 1933-1937, 2005.
2. Reits, E., Neijssen, J., Herberts, C., Benckhuijsen, W., Janssen, L., Drijfhout, J. W., and Neefjes, J. A major role for TPPII in trimming proteasomal degradation products for MHC class I antigen presentation., Immunity. 20: 495-506, 2004.
3. Seifert, U., Maranon, C., Shmueli, A., Desoutter, J. F., Wesoloski, L., Janek, K., Henklein, P., Diescher, S., Andrieu, M., de la Salle, H., Weinschenk, T., Schild, H., Laderach, D., Galy, A., Haas, G., Kloetzel, P. M., Reiss, Y., and Hosmalin, A. An essential role for tripeptidyl peptidase in the generation of an MHC class I epitope., Nature Immunology. 4: 375-9, 2003.
4. Rose, C., Vargas, F., Facchinetto, P., Bourgeat, P., Bambal, R. B., Bishop, P. B., Chan, S. M., Moore, A. N., Ganellin, C. R., and Schwartz, J. C. Characterization and inhibition of a cholecystokinin-inactivating serine peptidase, Nature. 380: 403-9, 1996.
5. Rockel, B., Peters, J., Kuhlmann, B., Glaeser, R. M., and Baumeister, W. A giant protease with a twist: the TPP II complex from Drosophila studied by electron microscopy, EMBO Journal. 21: 5979-84, 2002.
6. Tomkinson, B. Association and dissociation of the tripeptidyl-peptidase II complex as a way of regulating the enzyme activity, Archives of Biochemistry & Biophysics. 376: 275-80, 2000.
7. Wray, C. J., Tomkinson, B., Robb, B. W., and Hasselgren, P. O. Tripeptidyl-peptidase II expression and activity are increased in skeletal muscle during sepsis, Biochemical & Biophysical Research Communications. 296: 41-7, 2002.
8. Stavropoulou, V., Xie, J., Henriksson, M., Tomkinson, B., Imreh, S., and Masucci, M. G. Mitotic infidelity and centrosome duplication errors in cells overexpressing tripeptidyl-peptidase II, Cancer Research. 65: 1361-8, 2005.
9. Wang, S. C., Lin, S. H., Su, L. K., and Hung, M. C. Changes in BRCA2 expression during progression of the cell cycle, Biochemical & Biophysical Research Communications. 234: 247-51, 1997.

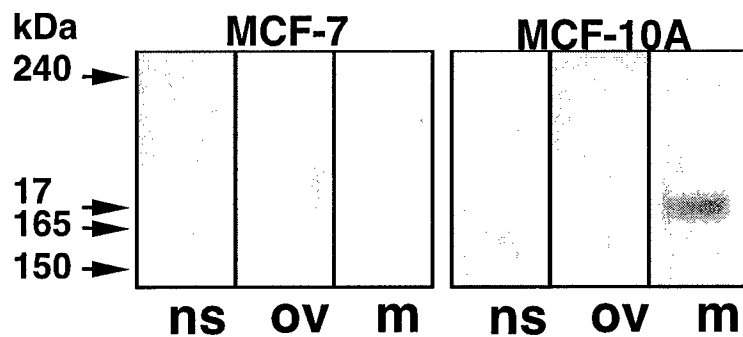
Cytosolic fractions



Membrane fractions



Nuclear fractions



ns - nonsynchronous; ov - overconfluent; m - mitotic

Figure 1. The pattern of TPP II subunits differs between subcellular compartments, between cells in distinct physiological state and between the cancerous and control cells (see also Table 1). Cytosolic, membrane and nuclear fractions were subjected to SDS-PAGE (6% acrylamide) and Western blotting, and the blots were probed with specific anti-TPP II antibodies.

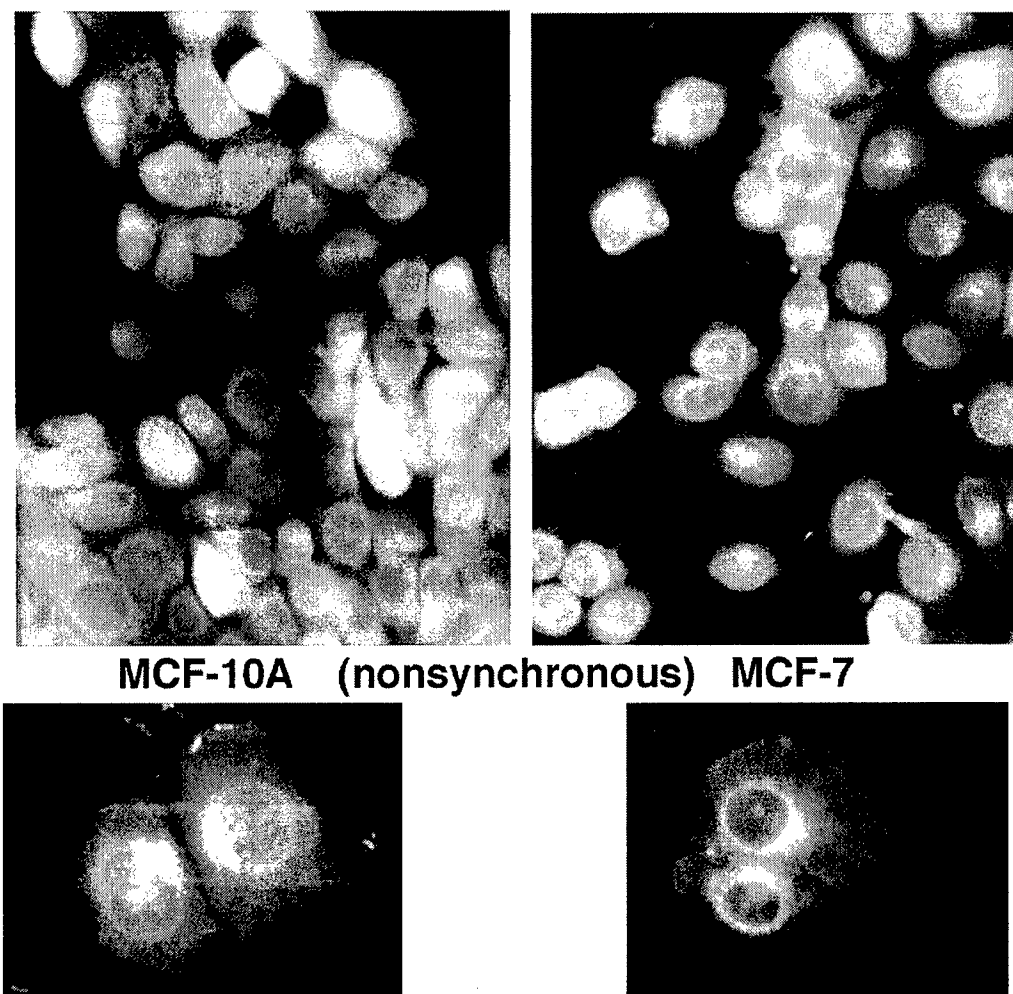


Figure 2. The subcellular localization and activity of TPP II differs between MCF7 and MCF10A cells. Nonsynchronous MCF10A (control) and MCF7 (cancerous) breast cells were incubated with fluorescent substrate of the TPP II AAF-CMAC. Top: fields of cells growing on coverslips (collected at magnification 400 x); bottom, close-up of cells just after cell division (collected at magnification 630x). The fluorescence of a free CMAC released from the substrate by peptidolytic activity of the TPP II was imaged under fluorescence microscope with the use of a blue filter. The fluorescence is visualized as white and shades of gray on a black background. The relative intensity of gray shading in both images was artificially brought to similar brightness and contrast for the convenience of direct comparison in the Figure. However, the relative intensity of fluorescence of MCF7 cells was several times lower than the intensity of fluorescence of MCF10A cells, as judged by the exposure times necessary to visualize the fluorescence of CMAC. Nevertheless, the relative fluorescence around the nuclear envelope, as compared with the fluorescence of the cytosol, seems to be more prominent in MCF7 than in MCF10A cells.

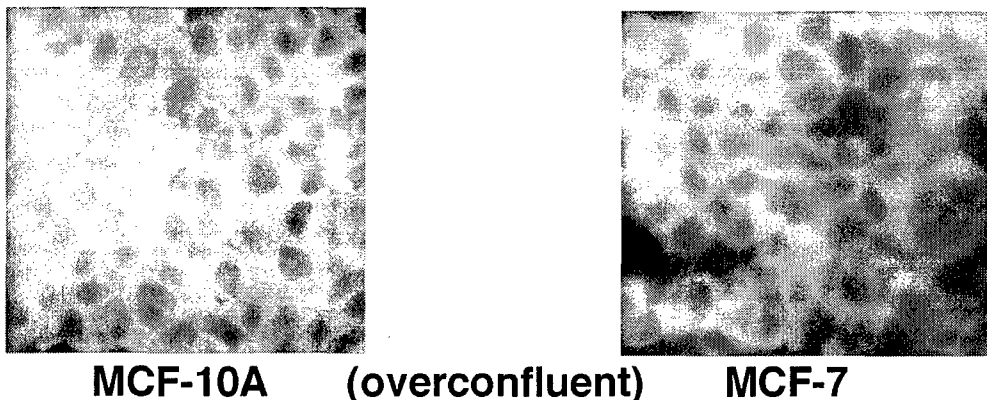


Figure 3. The intracellular activity of TPP II is relatively low in MCF7 and MCF10A cells at G_0 . Control and cancerous breast cells were incubated with fluorescent substrate of the TPP II AAF-CMAC. Only a relatively faint, dispersed fluorescence of free CMAC is visible in the cytosol of both types of cells. The dark ovals in the center of cells are nuclei, as was assessed with nucleic-acid staining fluorescent dye propidium iodide. The images were collected with 400x magnification.

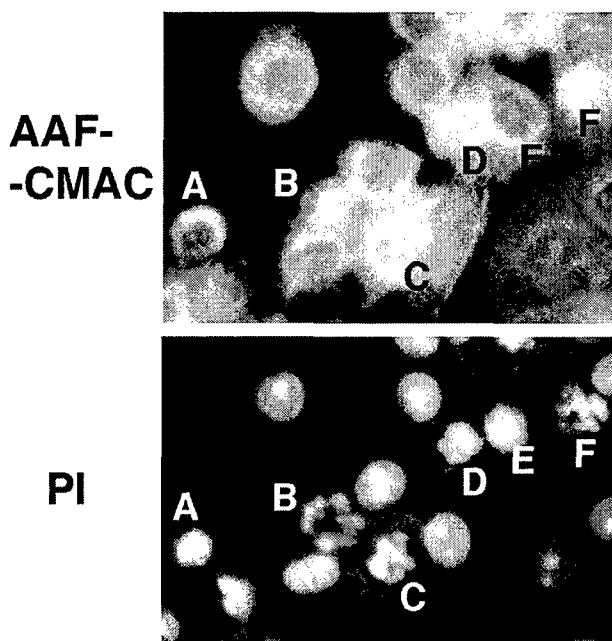


Figure 4. Active TPP II changes its subcellular localization depending on the stage of cell cycle. A gallery of MCF10A cells on different stages of mitosis is presented (images collected with 630x magnification). Top: cells treated with AAF-CMAC and fixed, bottom, the same cells stained with PI to visualize DNA. Examples of cells: A, E - chromatin condensed, CMAC fluorescence dispersed in cytosol and faintly bordering chromosomes; B, C, D, F – chromatin on early stages of condensation, CMAC fluorescence very strong and surrounding the chromatin.

APPENDICES

Abstract of the poster presented during the 12th Annual Symposium in Cancer Research in San Antonio (July 12, 2002, San Antonio, TX)

Cancer, proteases and proteolytic instability. *Pawel A. Osmulski, Xianzhi Jang, Bingnan Gu, Maria E Gaczynska. Department of Molecular Medicine, University of Texas Health Science Center at San Antonio, San Antonio, TX 78245.

Protein degradation, in concert with protein synthesis, governs the proper execution of metabolic processes in the cell. The large, intracellular proteases like anti-cancer drug target proteasome, a novel protease TPP II, tripeptidyl peptidase II (TPPII) or leucine aminopeptidase (LAP) play a key role among all proteolytic enzymes due to their diverse functions. The proteasome actions are essential for cell cycle regulation, turnover of transcription factors and antigen processing. Inhibition of proteasome leads to cell death and is utilized to kill tumor cells. However, there are strong indications that the other proteases may also constitute valuable anti-cancer drug targets. The postulated duties of TPP II include degradation of cell cycle related factors and, together with TPPII and LAP, further processing of antigenic peptides produced by proteasome. The collaboration of proteasome and other large proteases suggests the existence of a net of functional relationships between the executors of controlled proteolysis. We demonstrate here that proteolytic instability, which manifests in changing the equilibrium between the activities of large cytosolic proteases is one of the signs of neoplastic transformation in human breast cancer MCF-7 cells, as compared with non-cancerous MCF-10A cells. In the functional proteomics fashion we found prominent changes in activities of the enzymes, in their subunit composition and subcellular distribution. Specifically, we found that there is markedly less proteasomes in nuclei of the cancerous than control cells, and nuclei of cancer and control cells have dramatically different pattern of subunits of a natural proteasome activator. Since proteasome, TPP II, TPPII and LAP all take part in antigen processing, the changes may impair removal of transformed cells by the organism. Probing the role of large proteases in maintaining the proper advance of cell cycle we discovered that the predominantly cytosolic TPP II can be found in the nucleus. Interestingly, both nuclei and cytosol of cancer cells contain mostly overphosphorylated, unstable forms of the protease. We postulate that the nuclear localization of TPP II holds the key for dissecting its role in cell cycle progression.

Abstract of the poster presented during the Era of Hope DOD Breast Cancer Research Program Meeting (Orlando, September 25-28, 2002).

PROTEOLYTIC INSTABILITY IN BREAST CANCER CELLS

**Maria E Gaczynska, Xianzhi Jang, Bingnan Gu,
Pawel A. Osmulski**

Protein degradation, in concert with protein synthesis, governs the proper execution of metabolic processes in the cell. The large, intracellular proteases like anti-cancer drug target proteasome, a novel protease TPP II, tripeptidyl peptidase II (TPPII) or leucine aminopeptidase (LAP) play a key but poorly understood role among all proteolytic enzymes due to their diverse functions. The proteasome actions are essential for cell cycle regulation, turnover of transcription factors and antigen processing. Inhibition of proteasome leads to cell death and is utilized to kill tumor cells. However, there are strong indications that the other proteases may also constitute valuable anti-cancer drug targets. The postulated duties of TPP II include degradation of cell cycle related factors and, together with TPPII and LAP, further processing of antigenic peptides produced by proteasome. The collaboration of proteasome and other large proteases suggests the existence of a net of functional relationships between the executors of controlled proteolysis.

We show here that proteolytic instability, which manifests in changing the equilibrium between the activities of large cytosolic proteases is one of the signs of neoplastic transformation in human breast cancer MCF-7 cells, as compared with non-cancerous MCF-10A cells. To demonstrate the proteolytic instability we quantified the amount of enzymes with Western blotting, and determined their proteolytic activities with high-throughput methods using specific fluorogenic peptide substrates.

In the functional proteomics fashion we found prominent changes on both the functional level of activities and specificities of the enzymes, and the structural level of subunit composition, modifications and subcellular distribution. Specifically, we found that there is markedly less proteasomes in nuclei of the cancerous than control cells, and nuclei of cancer and control cells have dramatically different pattern of subunits of a natural proteasome activator. Since proteasome, TPP II, TPPII and LAP all take part in antigen processing, the changes may impair removal of transformed cells by the organism. Probing the role of large proteases in maintaining the proper advance of cell cycle we discovered that the predominantly cytosolic TPP II can be found in the nucleus, but this residence is much more pronounced in cancerous than in control cells. Interestingly, both nuclei and cytosol of cancer cells contain mostly overphosphorylated, unstable forms of the protease. We postulate that the nuclear localization of TPP II holds the key for dissecting the role of this protease in cell cycle progression.

Our findings show a fragment of potentially critical interactions between parts of the controlled proteolysis machinery. This web of interactions should be taken into account when anti-cancer drugs target single components of the whole system.

The U.S. Army Medical Research Materiel Command under DAMD17-01-1-0410 supported this work.

Abstract of the poster presented during the 2nd International Symposium on Cancer Research "Frontiers in Cancer Research: a Molecular Perspective" (San Antonio, October 12-14, 2002).

PROTEOLYTIC INSTABILITY IN BREAST CANCER CELLS

Pawel A. Osmulski, Xianzhi Jang, Bingnan Gu, Maria E. Gaczynska

University of Texas Health Science Center at San Antonio, Institute of Biotechnology,
15355 Lambda Drive, TX 78245

Protein degradation, in concert with protein synthesis, governs the proper execution of metabolic processes in the cell. The large, intracellular proteases like anti-cancer drug target proteasome, a novel protease TPP II, bleomycin hydrolase (BH), or leucine aminopeptidase (LAP) play a key but poorly understood role among all proteolytic enzymes due to their diverse functions. The proteasome actions are essential for cell cycle regulation, turnover of transcription factors and antigen processing. Inhibition of proteasome leads to cell death and is utilized to kill tumor cells. One of the synthetic proteasome inhibitors, a peptide boronate derivative PS-341 is already in clinical trials against multiple cancers, including breast cancer. However, there are strong indications that the other proteases may also constitute valuable anti-cancer drug targets. The postulated duties of TPP II include degradation of cell cycle related factors and, together with BH and LAP, further processing of antigenic peptides produced by proteasome. The collaboration of proteasome and other large proteases suggests the existence of a net of functional relationships between the executors of controlled proteolysis.

We show here that proteolytic instability, which manifests in changing the equilibrium between the activities of large cytosolic proteases is one of the signs of neoplastic transformation in human breast cancer MCF-7 cells, as compared with non-cancerous MCF-10A cells. To demonstrate the proteolytic instability we quantified the amount of enzymes with Western blotting, and determined their proteolytic activities with high-throughput methods using specific fluorogenic peptide substrates. In the functional proteomics fashion we found prominent changes on both the functional level of activities and specificities of the enzymes, and the structural level of subunit composition, modifications and subcellular distribution. Specifically, we found that immunoproteasomes, the specialized complexes especially well suited for antigen processing, are nearly absent in the cytosol of cancerous cells. Additionally, there is markedly less proteasomes in nuclei of the cancerous than control cells, and cancer and control cells have dramatically different pattern of subunits of a natural proteasome activator. We found that the new giant, predominantly cytosolic protease TPP II is found in the nucleus of cells arrested in pseudo-mitosis with nocodazole, however only in control and not in cancerous cells. Interestingly, there is generally much less TPP II-related activity in cancerous than in control cells and cancer cells contain mostly overphosphorylated, unstable forms of the protease.

Our findings show a fragment of interactions between parts of the controlled proteolysis machinery critical for antigen processing and cell cycle regulation. This web of interactions should be taken into account when anti-cancer drugs target single components of the whole system.

Abstract of the poster presented on the 13th Annual Symposium on Cancer Research in San Antonio and South Texas (November 11th, 2004)

Synergistic action of inhibitors of large cytosolic proteases on breast cancer cells.

*Gaczynska M., Jankowska E., Osmulski P.A., University of Texas Health Science Center at San Antonio, Department of Molecular Medicine, Institute of Biotechnology, San Antonio, TX 78245-3207.

We showed that breast cancer MCF-7 cells possess a distinct regulation of proteolysis executed by the TPP II when compared with non-cancerous MCF-10A cells. The apparent lower total activity of the large cytosolic protease TPP II in MCF-7 cells and only weak changes in subcellular localization may constitute an important link between the overall efficiency of cell division and nuclear and cytosolic proteolysis. Regulation of the assembly of the large and small forms of TPP II is accomplished through a complex phosphorylation pattern of their subunits. Moreover, it seems that the phosphorylation also controls subcellular localization of the TPP II and ultimately its fate. The cellular distribution of the TPP II, similarly to the best known large intracellular protease, the proteasome, is not limited to cytosol, however the most of the both proteases resides in this compartment. On the basis of our data we suspect that TPP II constitutes an important player in cellular protein turnover and in regulation of cell cycle. Its distinct properties in the control and cancerous cells strongly suggest that the TPP II may represent an attractive drug target and a marker of physiological state of the cells. Since it has been long suspected that both proteasome and the TPP II may share some of their functions, we tested the viability of the cancerous and control cells treated with inhibitors of (1) the proteasome, (2) the TPP II, and (3) both the inhibitors combined. The results of these tests are very encouraging. High doses of either the TPP II or proteasome inhibitors are invariably toxic to the cells. However, we determined that a combination of low doses of both the inhibitors effectively kills the cancerous cells allowing the noncancerous cells to recover. This result point at a potential practical use of mixed-inhibitor therapy and underlines the importance of comprehensive understanding of cellular controlled proteolysis.

Abstract of a poster to be presented during the Era of Hope DOD Breast Cancer Research Program Meeting (Philadelphia, June 8-11, 2005).

INHIBITORS OF LARGE CYTOSOLIC PROTEASES ACT SYNERGISTICALLY TO KILL BREAST CANCER CELLS.

Maria Gaczynska and Paweł A. Osmulski

University of Texas Health Science Center at San Antonio, Department of Molecular Medicine, Institute of Biotechnology, San Antonio, TX 78245-3207

E-mail: gaczynska@uthscsa.edu

Proper regulation of cell division and cell differentiation are the major factors preventing the neoplastic growth. Proteolysis is one of the controlling mechanisms of these processes. The giant multifunctional enzyme named the proteasome is the most important executor of proteolysis in human cells, and a recently acknowledged target for anticancer drugs. Inhibition of the proteasomal actions leads to apoptosis, and cancer cells are apparently more susceptible to undergo programmed death induced by proteasome inhibitors than normal cells. Still, normal cells are harmed by the inhibitors and cancer cells do eventually adapt to the persistent partial inhibition of the proteasome. Therefore, we turned our attention to other giant enzymes supplementing the proteasome in intracellular proteolysis: the TPP II (M1t), discovered in our laboratory, and tripeptidyl peptidase II (TPPII). We decided to test mixtures of inhibitors targeting the proteases on breast cancer and control cultured cells. First, we planned to test if any of the mixtures of inhibitors will show a synergistic effect on the cell survival. Second, we hoped to detect differences in the response of cancerous and noncancerous cells to the treatments.

We analyzed the viability of human breast carcinoma cultured cells MCF-7 and non-cancerous breast cells MCF-10A treated with inhibitors of (1) the proteasome, (2) the TPP II and TPPII, and (3) both the inhibitors combined. We chose a peptide boronic acid derivative carbobenzoxy-LeuLeuLeu-B(OH)2 (MG262) and AlaAlaPhe-chloro methylketone (AAF-CMK) as inhibitors. MG262 is a highly specific, high-affinity inhibitor of the proteasome and a close homologue of the drug bortezomib approved to treat multiple myeloma and in trials for breast and other cancers. AAF-CMK competitively restrains the proteolytic activity of the TPP II and TPPII. We tested an array of several concentrations of the individual inhibitors or their combinations. We determined viability of cells cultured for up to 48 hours in the presence of the inhibitor(s) and analyzed activities of the proteases in cell extracts.

The results of these tests are very encouraging. The treatment with the mixture of inhibitors led to a stronger and faster inhibition of the proteasomal activity than any of the inhibitors acting alone. Only a very limited recovery of the proteasomal activity was observed, especially after treatment with the mixtures. Moreover, we determined that a combination of low doses of both the inhibitors more effectively kills the cancerous cells allowing the noncancerous cells to recover. This result points at a potential practical use of mixed-inhibitor therapy and underlines the importance of comprehensive understanding of cellular controlled proteolysis.